First Measurement of Muon Neutrino Charged Current Quasielastic (CCQE) Double Differential Cross Section

PRD81(2010)092005

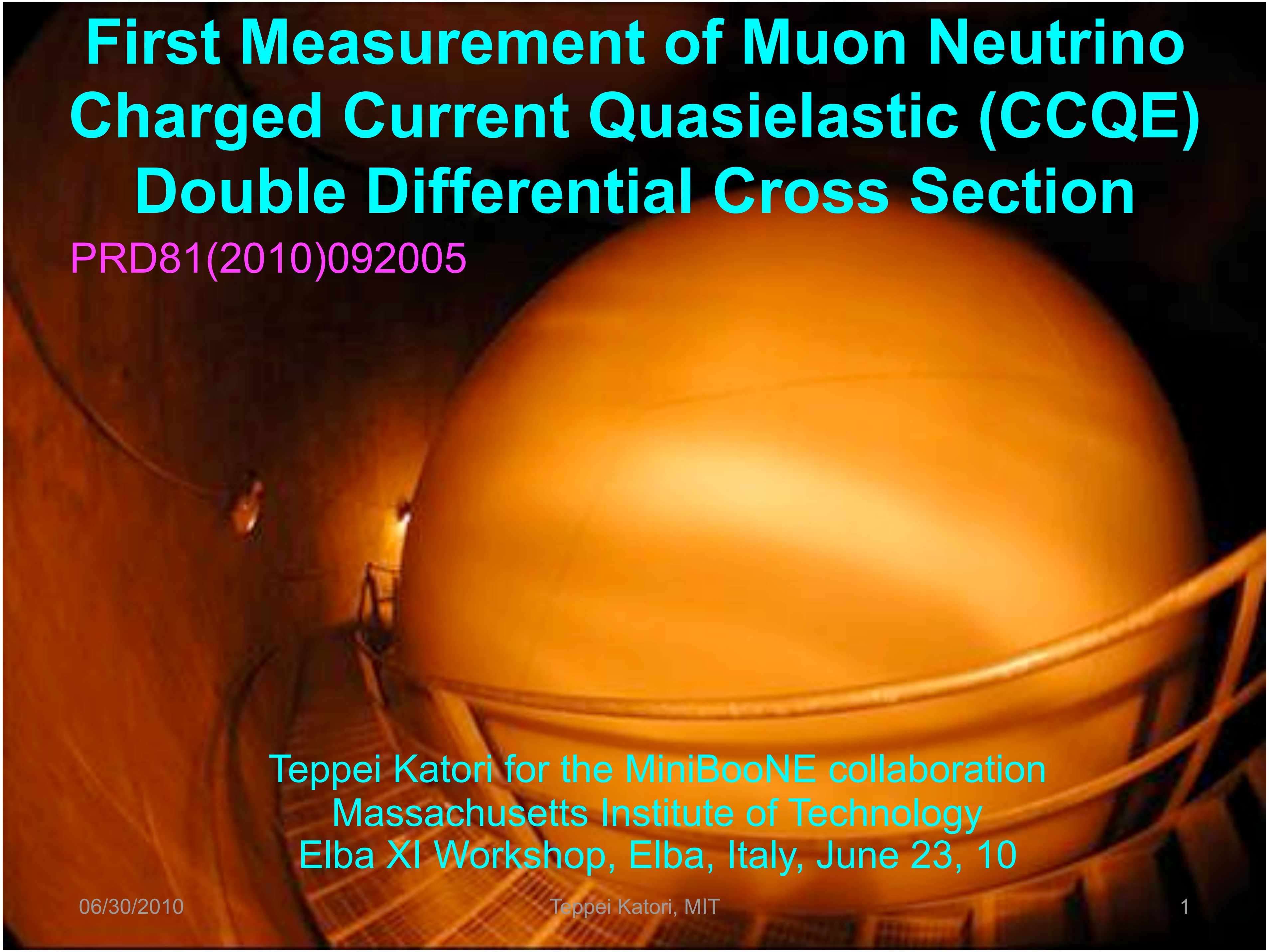

Teppei Katori for the MiniBooNE collaboration
Massachusetts Institute of Technology
Elba XI Workshop, Elba, Italy, June 23, 10

First Measurement of Muon Neutrino Charged Current Quasielastic (CCQE) Double Differential Cross Section

PRD81(2010)092005

outline

0. NuInt09 summary
1. Booster neutrino beamline
2. MiniBooNE detector
3. CCQE events in MiniBooNE
4. CC1π background constraint
5. CCQE M_A^{eff}-κ shape-only fit
6. CCQE absolute cross section
7. Conclusion

0. NuInt09 summary

NuInt09, May18-22, 2009, Sitges, Spain
All talks proceedings are available on online (open access),
http://proceedings.aip.org/proceedings/confproceed/1189.jsp

NuInt09 MiniBooNE results
In NuInt09, MiniBooNE had 6 talks and 2 posters

1. charged current quasielastic (CCQE) cross section measurement
   by Teppei Katori, PRD81(2010)092005
2. neutral current elastic (NCE) cross section measurement
   by Denis Perevalov, paper in preparation
3. neutral current π^o production (NCπ^o) cross section measurement (ν and anti-ν)
   by Colin Anderson, PRD81(2010)013005
4. charged current single pion production (CCπ^+) cross section measurement
   by Mike Wilking, paper in preparation
5. charged current single π^o production (CCπ^o) measurement
   by Bob Nelson, paper in preparation
6. improved CC1π^+ simulation in NUANCE generator
   by Jarek Novak
7. CCπ^+/CCQE cross section ratio measurement
   by Steve Linden, PRL103(2009)081801
8. anti-νCCQE measurement
   by Joe Grange, paper in preparation

0. NuInt09 summary

NuInt09, May18-22, 2009, Sitges, Spain
All talks proceedings are available on online (open access),
http://proceedings.aip.org/proceedings/confproceed/1189.jsp

NuInt09 MiniBooNE results
In NuInt09, MiniBooNE had 6 talks and 2 posters

1. charged current quasielastic (CCQE) cross section measurement
   by Teppei Katori, PRD81(2010)092005
2. neutral current elastic (NCE) cross section measurement
   by Denis Perevalov, paper in preparation
3. neutral current π^o production (NCπ^o) cross section m
   by Colin Anderson, PRD81(2010)013005
4. charged current single pion production (CCπ^+) cross
   by Mike Wilking, paper in preparation
5. charged current single π^o production (CCπ^o) measure
   by Bob Nelson, paper in preparation
6. improved CC1π^+ simulation in NUANCE generator
   by Jarek Novak
7. CCπ^+/CCQE cross section ratio measurement
   by Steve Linden, PRL103(2009)081801
8. anti-νCCQE measurement
   by Joe Grange, paper in preparation

$$\nu_\mu + n \rightarrow p + \mu^-$$

$$(\nu_\mu + {}^{12}C \rightarrow X + \mu^-)$$

CCQE double differential cross section

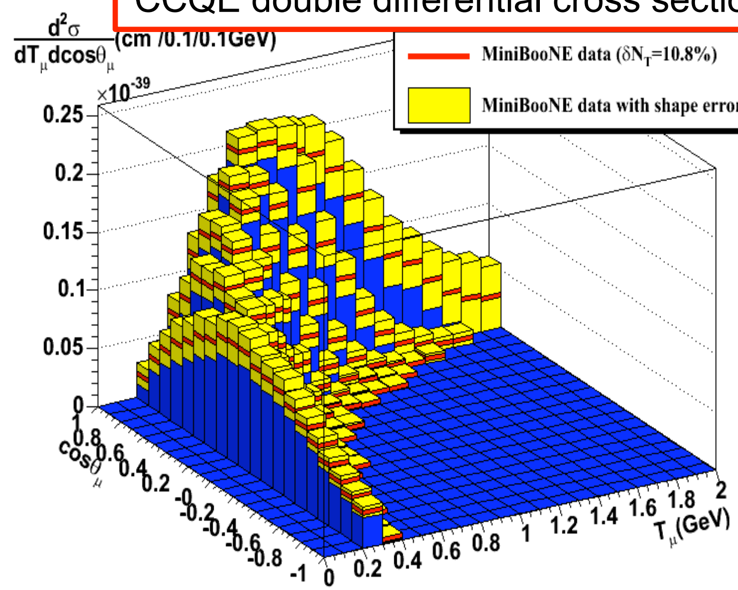

by Denis Perevalov

0. NuInt09 summary

NuInt09, May18-22, 2009, Sitges, Spain

All talks proceedings are available on online (open access),

http://proceedings.aip.org/proceedings/confproceed/1189.jsp

NuInt09 MiniBooNE results

In NuInt09, MiniBooNE had 6 talks and 2 posters

1. charged current quasielastic (CCQE) cross section measurement
   by Teppei Katori, PRD81(2010)092005
2. neutral current elastic (NCE) cross section measurement
   by Denis Perevalov, paper in preparation
3. neutral current π^o production (NCπ^o) cross section
   by Colin Anderson, PRD81(2010)013005
4. charged current single pion production (CCπ^+)
   by Mike Wilking, paper in preparation
5. charged current single π^o production (CCπ^o) m
   by Bob Nelson, paper in preparation
6. improved CC1π^+ simulation in NUANCE gene
   by Jarek Novak
7. CCπ^+/CCQE cross section ratio measurement
   by Steve Linden, PRL103(2009)081801
8. anti-νCCQE measurement
   by Joe Grange, paper in preparation

$$\nu_\mu + p \rightarrow \nu_\mu + p$$

$$\nu_\mu + n \rightarrow \nu_\mu + n$$

Flux-averaged NCE p+n differential cross section

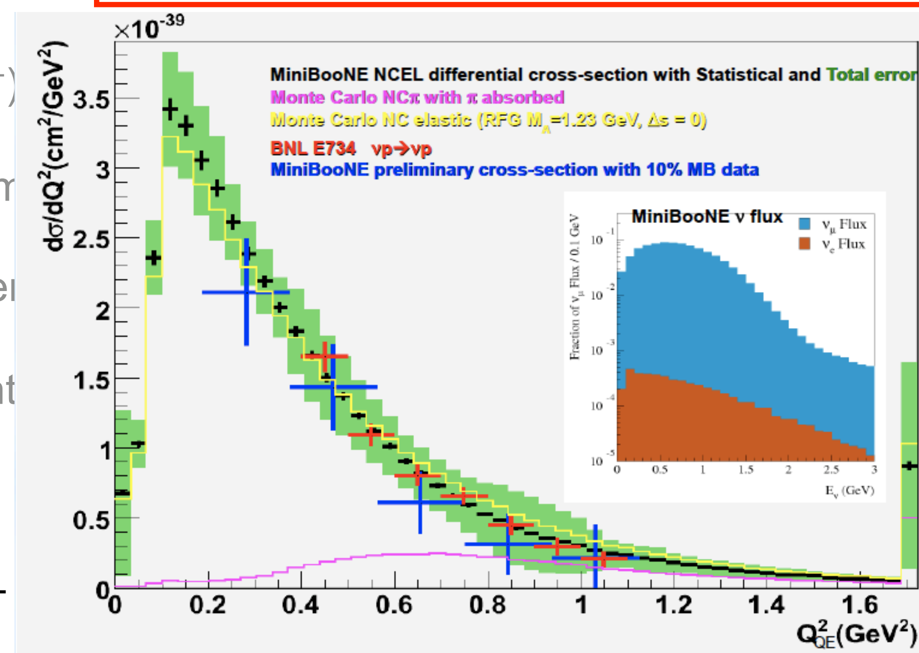

by Colin Anderson

0. NuInt09 summary

NuInt09, May18-22, 2009, Sitges, Spain
All talks proceedings are available on online (open access),
http://proceedings.aip.org/proceedings/confproceed/1189.jsp

NuInt09 MiniBooNE results
In NuInt09, MiniBooNE had 6 talks and 2 posters

1. charged current quasielastic (CCQE) cross section measurement
   by Teppei Katori, PRD81(2010)092005
2. neutral current elastic (NCE) cross section measurement
   by Denis Perevalov, paper in preparation
3. neutral current π^o production (NCπ^o) cross section measurement (ν and anti-ν)
   by Colin Anderson, PRD81(2010)013005
4. charged current single pion production (CCπ^+) cross section
   by Mike Wilking, paper in preparation
5. charged current single π^o production (CCπ^o) measurement
   by Bob Nelson, paper in preparation
6. improved CC1π^+ simulation in NUANCE generator
   by Jarek Novak
7. CCπ^+/CCQE cross section ratio measurement
   by Steve Linden, PRL103(2009)081801
8. anti-νCCQE measurement
   by Joe Grange, paper in preparation

$$\nu_\mu + N \rightarrow \nu_\mu + \Delta^o \rightarrow \nu_\mu + N + \pi^o$$

$$\nu_\mu + A \rightarrow \nu_\mu + A + \pi^o$$

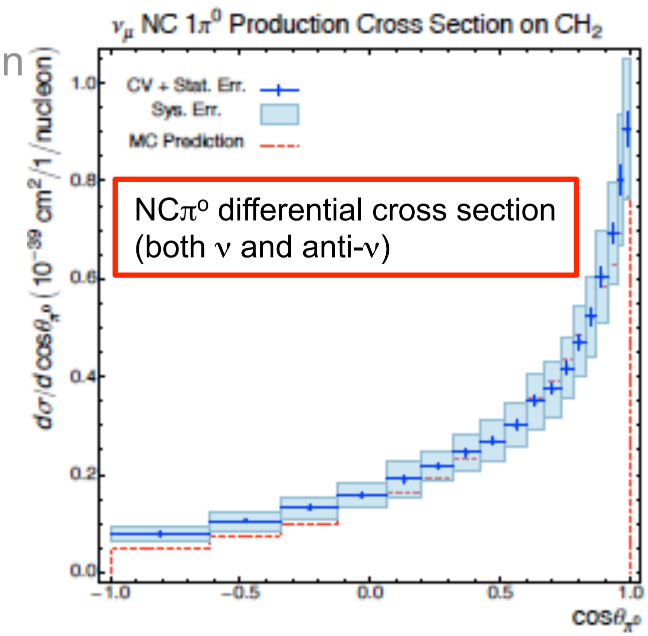

by Mike Wilking

0. NuInt09 summary

NuInt09, May18-22, 2009, Sitges, Spain
All talks proceedings are available on online (open access),
http://proceedings.aip.org/proceedings/confproceed/1189.jsp

NuInt09 MiniBooNE results
In NuInt09, MiniBooNE had 6 talks and 2 posters

1. charged current quasielastic (CCQE) cross section measurement
   by Teppei Katori, PRD81(2010)092005
2. neutral current elastic (NCE) cross section measurement
   by Denis Perevalov, paper in preparation
3. neutral current π^o production (NCπ^o) cross section
   by Colin Anderson, PRD81(2010)013005
4. charged current single pion production (CCπ^+) cross section measurement
   by Mike Wilking, paper in preparation
5. charged current single π^o production (CCπ^o) me
   by Bob Nelson, paper in preparation
6. improved CC1π^+ simulation in NUANCE genera
   by Jarek Novak
7. CCπ^+/CCQE cross section ratio measurement
   by Steve Linden, PRL103(2009)081801
8. anti-νCCQE measurement
   by Joe Grange, paper in preparation

$$\nu_\mu + p(n) \rightarrow \mu + \Delta^{+(+)} \rightarrow \mu + p(n) + \pi^+$$
$$\nu_\mu + A \rightarrow \mu + A + \pi^+$$

double differential cross section
(both pion and muon)

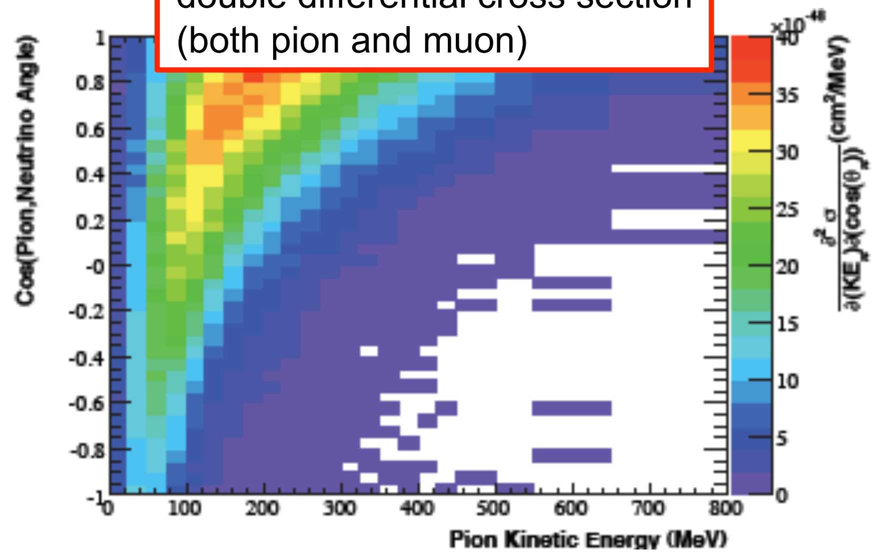

by Bob Nelson

0. NuInt09 summary

NuInt09, May18-22, 2009, Sitges, Spain
All talks proceedings are available on online (open access),
http://proceedings.aip.org/proceedings/confproceed/1189.jsp

NuInt09 MiniBooNE results
In NuInt09, MiniBooNE had 6 talks and 2 posters

1. charged current quasielastic (CCQE) cross section measur
   by Teppei Katori, PRD81(2010)092005
2. neutral current elastic (NCE) cross section measurement
   by Denis Perevalov, paper in preparation
3. neutral current π^o production (NCπ^o) cross section measure
   by Colin Anderson, PRD81(2010)013005
4. charged current single pion production (CCπ^+) cross sectio
   by Mike Wilking, paper in preparation
5. charged current single π^o production (CCπ^o) measurement
   by Bob Nelson, paper in preparation
6. improved CC1π^+ simulation in NUANCE generator
   by Jarek Novak
7. CCπ^+/CCQE cross section ratio measurement
   by Steve Linden, PRL103(2009)081801
8. anti-νCCQE measurement
   by Joe Grange, paper in preparation

$$\nu_\mu + n \rightarrow \mu + \Delta^+ \rightarrow \mu + p + \pi^o$$

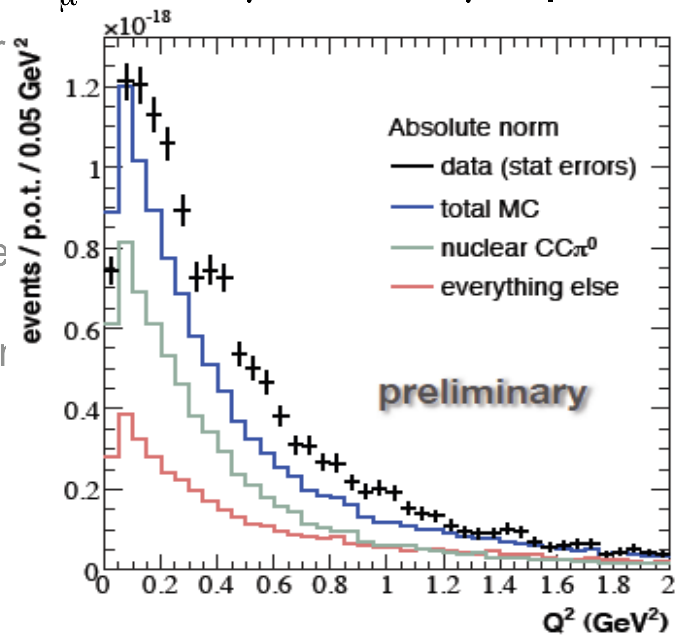

CCπ^o Q2 distribution
(paper will include absolute cross section)

by Jarek Novak

0. NuInt09 summary

NuInt09, May18-22, 2009, Sitges, Spain
All talks proceedings are available on online (open access),
http://proceedings.aip.org/proceedings/confproceed/1189.jsp

NuInt09 MiniBooNE results
In NuInt09, MiniBooNE had 6 talks and 2 posters

1. charged current quasielastic (CCQE) cross section measurement
   by Teppei Katori, PRD81(2010)092005
2. neutral current elastic (NCE) cross section measurement
   by Denis Perevalov, paper in preparation
3. neutral current π^o production (NCπ^o) cross section measurement (ν and anti-ν)
   by Colin Anderson, PRD81(2010)013005
4. charged current single pion production (CCπ^+) cross section measure[ment]
   by Mike Wilking, paper in preparation
5. charged current single π^o production (CCπ^o) measu[rement]
   by Bob Nelson, paper in preparation
6. improved CC1π^+ simulation in NUANCE generator
   by Jarek Novak
7. CCπ^+/CCQE cross section ratio measurement
   by Steve Linden, PRL103(2009)081801
8. anti-νCCQE measurement
   by Joe Grange, paper in preparation

$M_A^{1\pi}$ fit with Q^2 distribution for various nuclear models

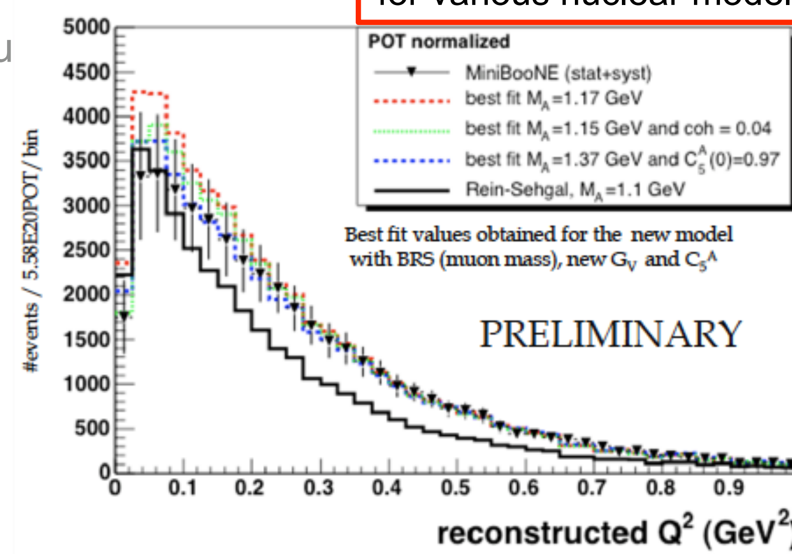

0. NuInt09 summary

by Steve Linden

picture wanted

NuInt09, May18-22, 2009, Sitges, Spain
All talks proceedings are available on online (open access),
http://proceedings.aip.org/proceedings/confproceed/1189.jsp

NuInt09 MiniBooNE results
In NuInt09, MiniBooNE had 6 talks and 2 posters

1. charged current quasielastic (CCQE) cross section
   by Teppei Katori, PRD81(2010)092005
2. neutral current elastic (NCE) cross section measure
   by Denis Perevalov, paper in preparation
3. neutral current π^o production (NCπ^o) cross section n
   by Colin Anderson, PRD81(2010)013005
4. charged current single pion production (CCπ^+) cross
   by Mike Wilking, paper in preparation
5. charged current single π^o production (CCπ^o) measu
   by Bob Nelson, paper in preparation
6. improved CC1π^+ simulation in NUANCE generator
   by Jarek Novak
7. CCπ^+/CCQE cross section ratio measurement
   by Steve Linden, PRL103(2009)081801
8. anti-νCCQE measurement
   by Joe Grange, paper in preparation

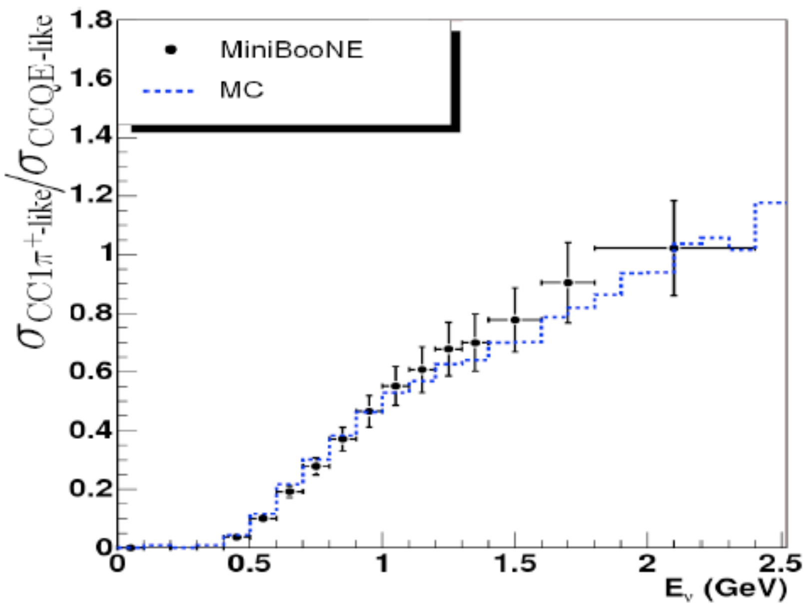

CCπ^+like/CCQElike cross section ratio by Joe Grange

0. NuInt09 summary

NuInt09, May18-22, 2009, Sitges, Spain

All talks proceedings are available on online (open access),

http://proceedings.aip.org/proceedings/confproceed/1189.jsp

NuInt09 MiniBooNE results

In NuInt09, MiniBooNE had 6 talks and 2 posters

1. charged current quasielastic (CCQE) cross section measurement by Teppei Katori, PRD81(2010)092005
2. neutral current elastic (NCE) cross section measurement by Denis Perevalov, paper in preparation
3. neutral current π^o production (NCπ^o) cross section measurement by Colin Anderson, PRD81(2010)013005
4. charged current single pion production (CCπ^+) cross section by Mike Wilking, paper in preparation
5. charged current single π^o production (CCπ^o) measurement by Bob Nelson, paper in preparation
6. improved CC1π^+ simulation in NUANCE generator by Jarek Novak
7. CCπ^+/CCQE cross section ratio measurement by Steve Linden, PRL103(2009)081801
8. anti-νCCQE measurement by Joe Grange, paper in preparation

$$\bar{\nu}_\mu + p \to n + \mu^+$$

$$\begin{pmatrix} \bar{\nu}_\mu + {}^{12}C \to X + \mu^+ \\ \bar{\nu}_\mu + {}^{1}H \to n + \mu^+ \end{pmatrix}$$

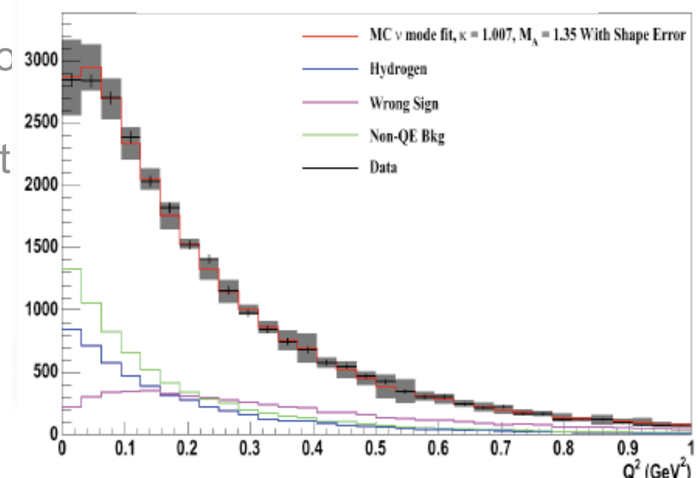

anti-νCCQE Q^2 distribution

by everyone

0. NuInt09 summary

NuInt09, May18-22, 2009, Sitges, Spain
All talks proceedings are available on online (open access),
http://proceedings.aip.org/proceedings/confproceed/1189.jsp

Some realizations from NuInt09

1. Neutrino cross section measurements are the urgent program, mainly, because of their relationship with neutrino oscillation measurements.
2. Importance to use the better models for neutrino interaction generators
3. Importance to provide data with the form available for theorists, this includes,
   i) detector efficiency is corrected
   ii) free from reconstruction biases (data as a function of measured quantities)
   iii) free from model dependent background subtraction

e.g.) MC comparison of double differential cross section of NCπ^o production with Eν=0.5GeV, angle=60^o

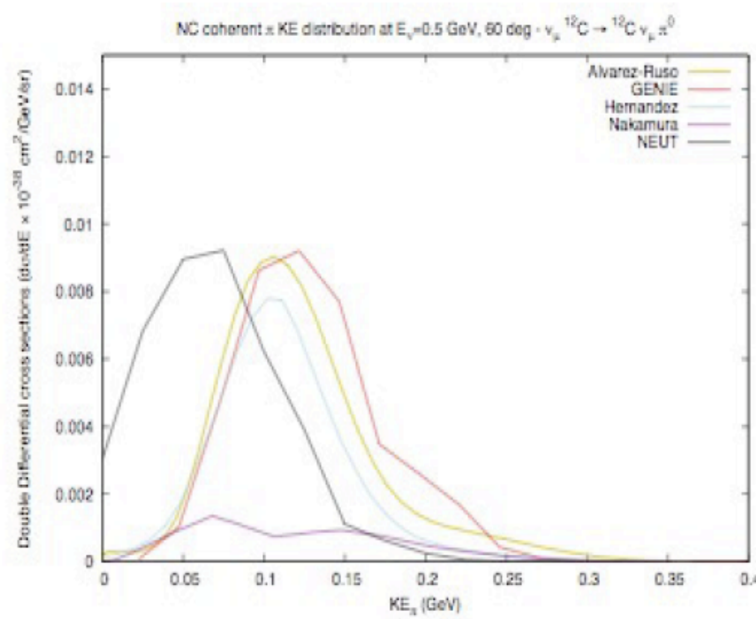

1. Booster neutrino beamline

2. MiniBooNE detector

3. CCQE events in MiniBooNE

4. CC1π background constraint

5. CCQE M_A^{eff}-κ shape-only fit

6. CCQE absolute cross section

7 Conclusion

MiniBooNE collaboration,
PRD79(2009)072002

1. Booster Neutrino Beamline

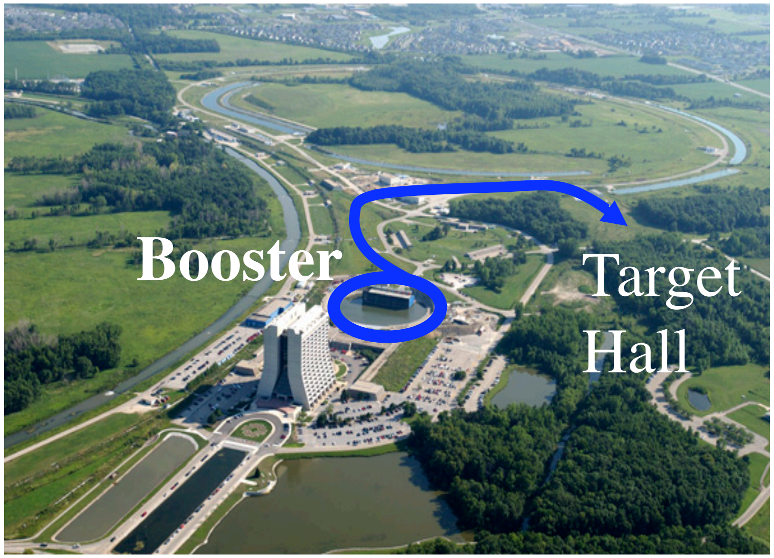

MiniBooNE extracts 8.9 GeV/c momentum proton beam from the Booster

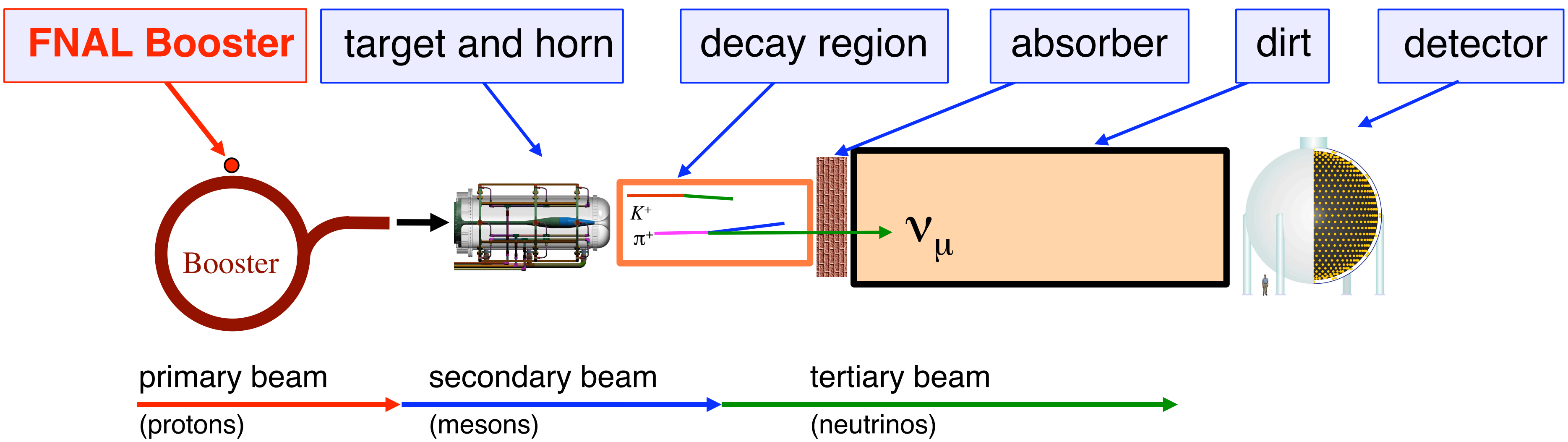

MiniBooNE collaboration,
PRD79(2009)072002

1. Booster Neutrino Beamline

Magnetic focusing horn

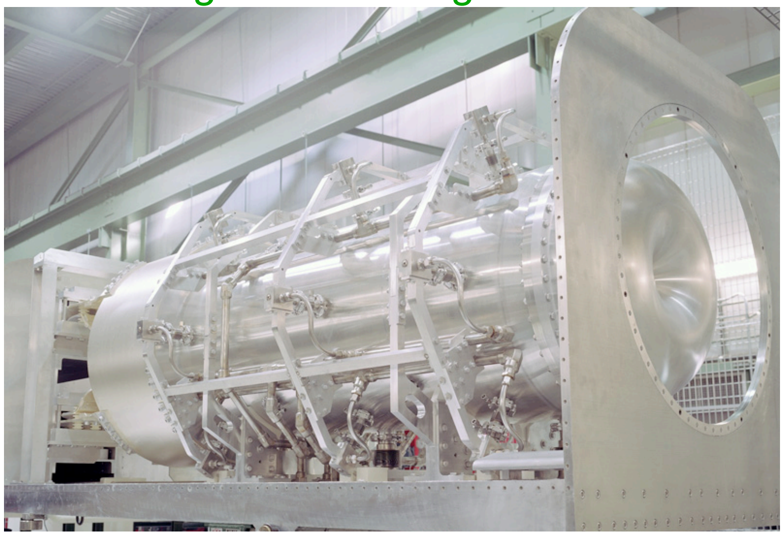

Protons are delivered to a beryllium target in a magnetic horn
(flux increase ~6 times)

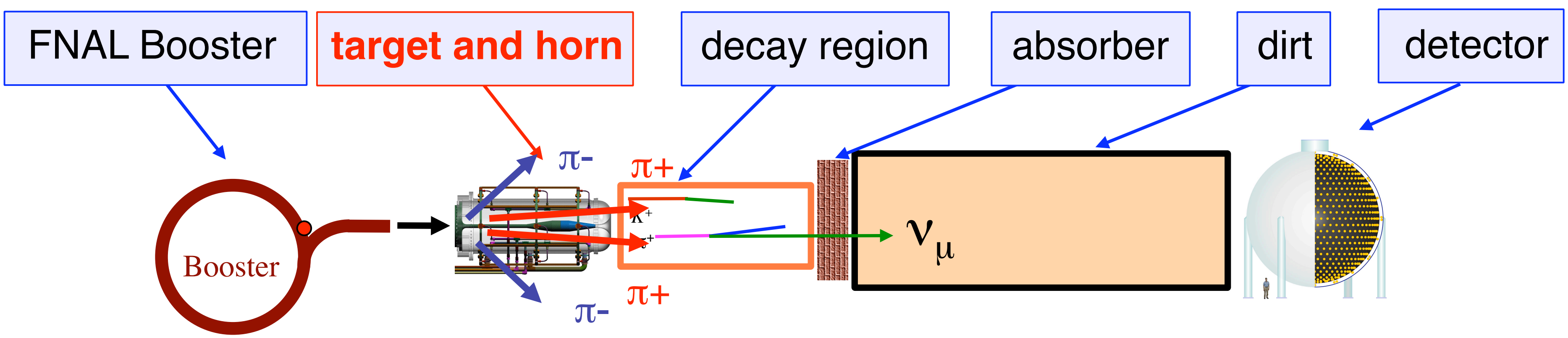

primary beam
(protons)

secondary beam
(mesons)

tertiary beam
(neutrinos)

MiniBooNE collaboration,
PRD79(2009)072002

1. Booster Neutrino Beamline

Modeling of meson production is based on the measurement done by HARP collaboration

- Identical, but 5% λ Beryllium target
- 8.9 GeV/c proton beam momentum

HARP collaboration,
Eur.Phys.J.C52(2007)29

HARP experiment (CERN)

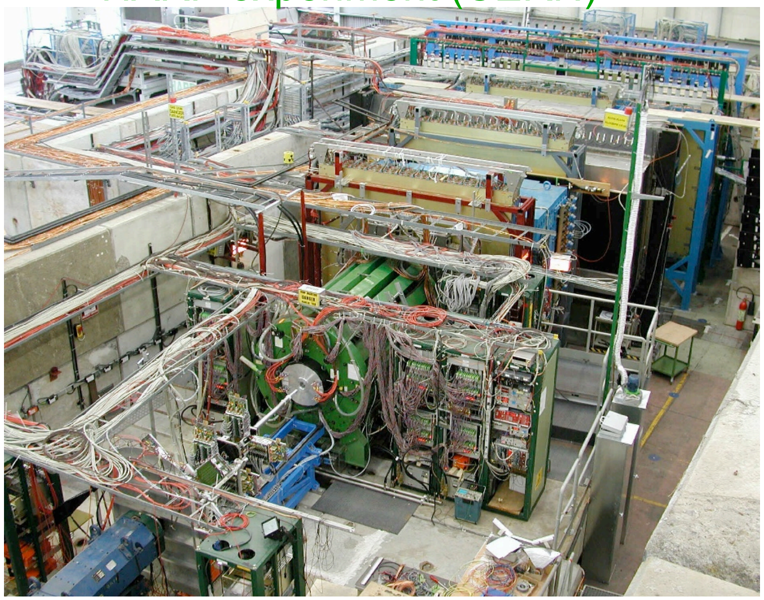

Booster neutrino beamline pion kinematic space

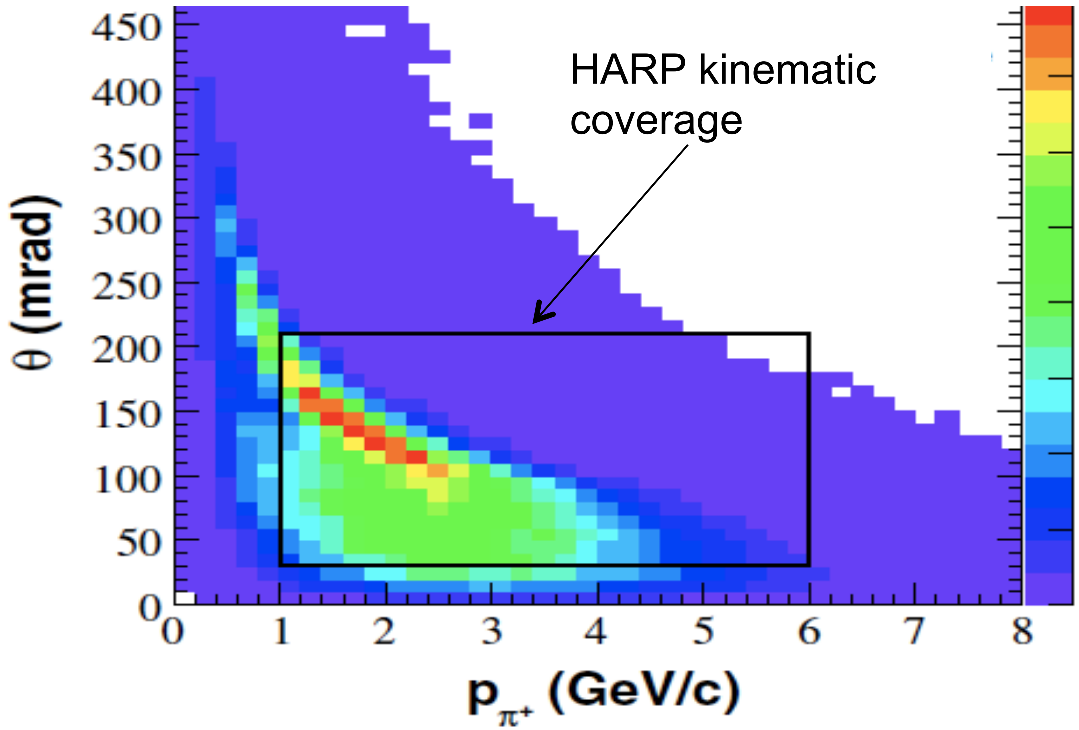

Majority of pions create neutrinos in MiniBooNE are directly measured by HARP (>80%)

MiniBooNE collaboration,
PRD79(2009)072002

1. Booster Neutrino Beamline

HARP experiment (CERN)

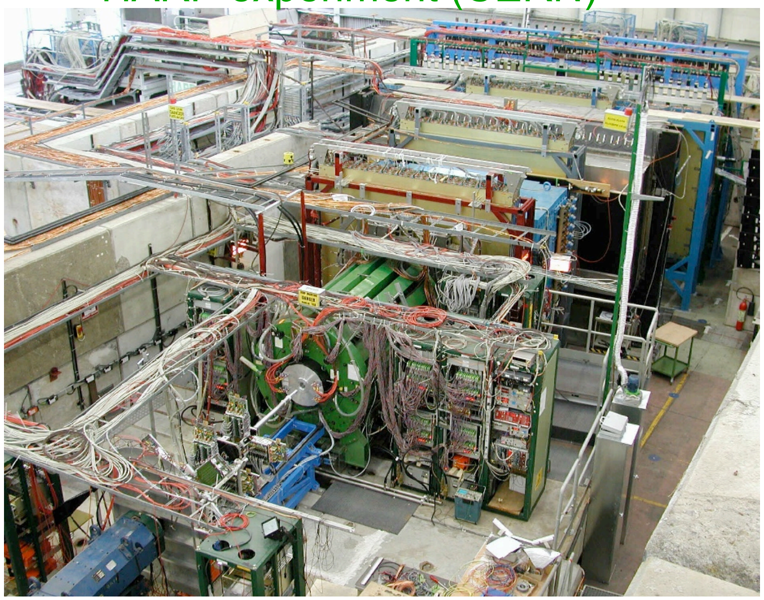

Modeling of meson production is based on the measurement done by HARP collaboration
- Identical, but 5% λ Beryllium target
- 8.9 GeV/c proton beam momentum

HARP collaboration,
Eur.Phys.J.C52(2007)29

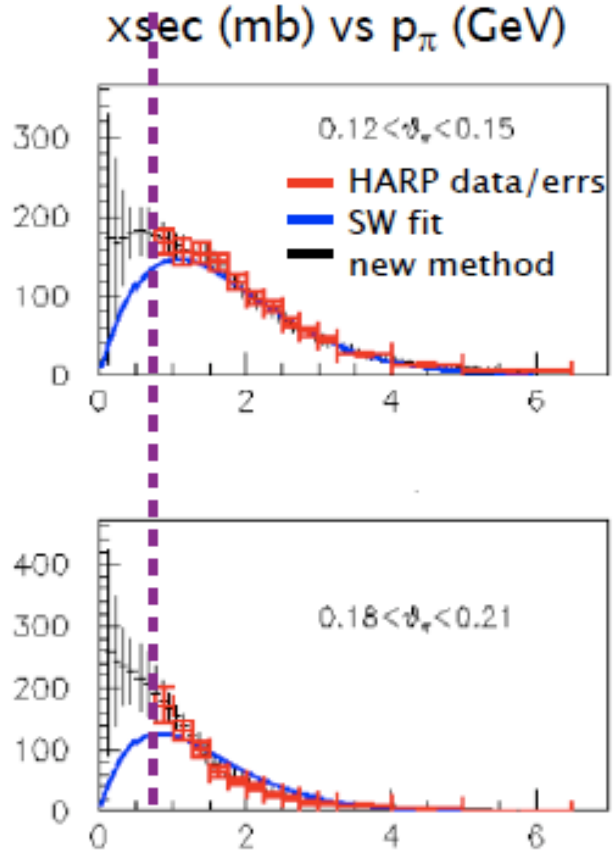

HARP data with 8.9 GeV/c proton beam momentum

The error on the HARP data (~7%) directly propagates.
The neutrino flux error is the dominant source of normalization error for an absolute cross section in MiniBooNE.

MiniBooNE collaboration,
PRD79(2009)072002

1. Booster Neutrino Beamline

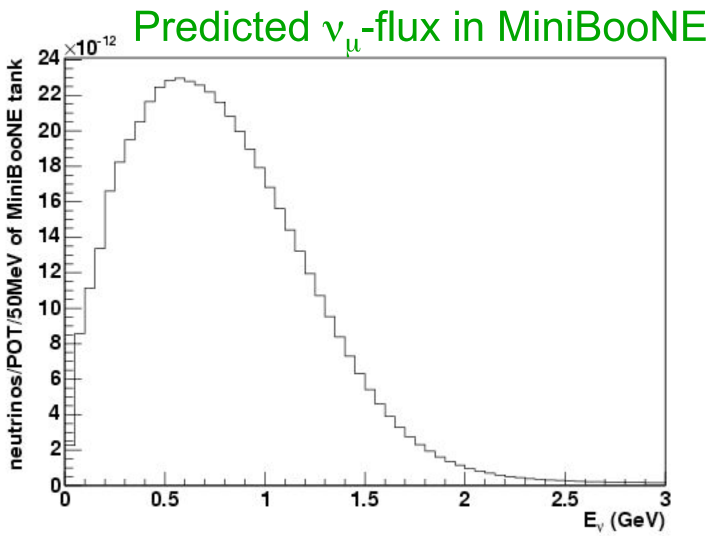

The decay of mesons make the neutrino beam. The neutrino beam is dominated by ν_μ (93.6%), of this, 96.7% is made by π^+-decay

$$\pi^+ \rightarrow \mu^+ + \nu_\mu$$

For all MiniBooNE cross section measurements, neutrino flux prediction is not tuned from our neutrino measurement data.

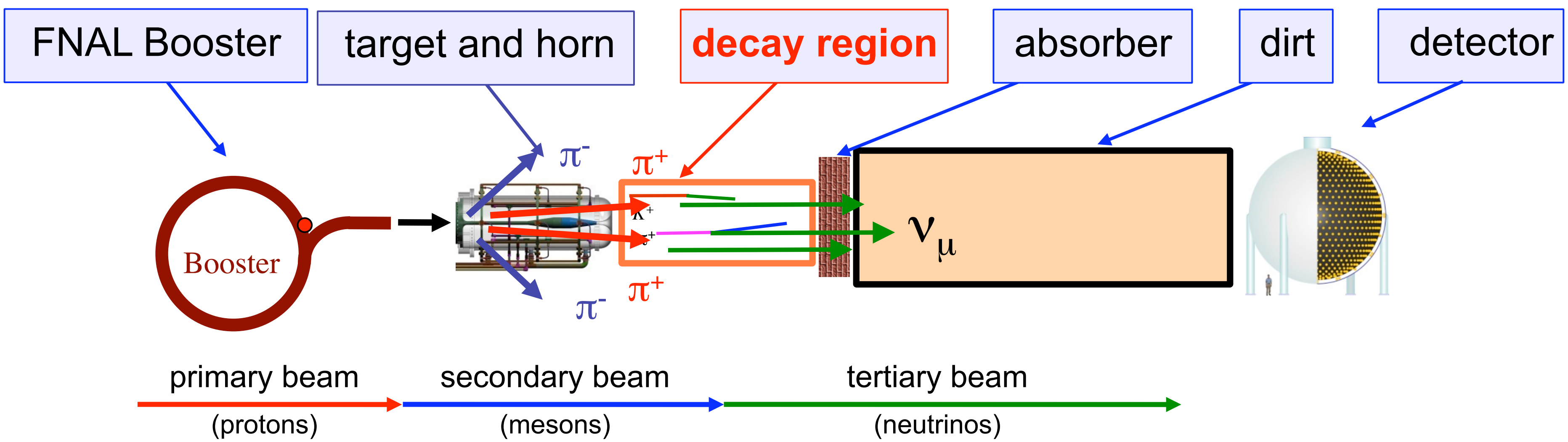

1. Booster neutrino beamline

2. MiniBooNE detector

3. CCQE events in MiniBooNE

4. CC1π background constraint

5. CCQE M_A^{eff}-κ shape-only fit

6. CCQE absolute cross section

7 Conclusion

MiniBooNE collaboration,
NIM.A599(2009)28

2. MiniBooNE detector

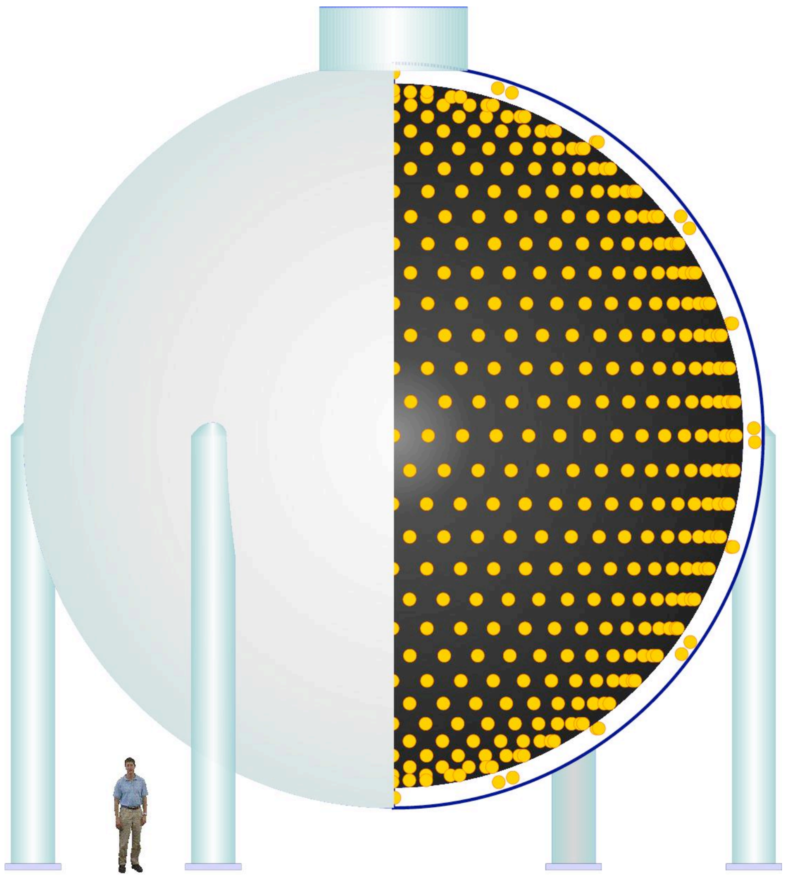

The MiniBooNE Detector

- 541 meters downstream of target
- 3 meter overburden
- 12 meter diameter sphere

  (10 meter “fiducial” volume)
- Filled with 800 t of pure mineral oil (CH_2)

  (Fiducial volume: 450 t)
- 1280 inner phototubes,
- 240 veto phototubes

  Simulated with a GEANT3 Monte Carlo

MiniBooNE collaboration,
NIM.A599(2009)28

2. MiniBooNE detector

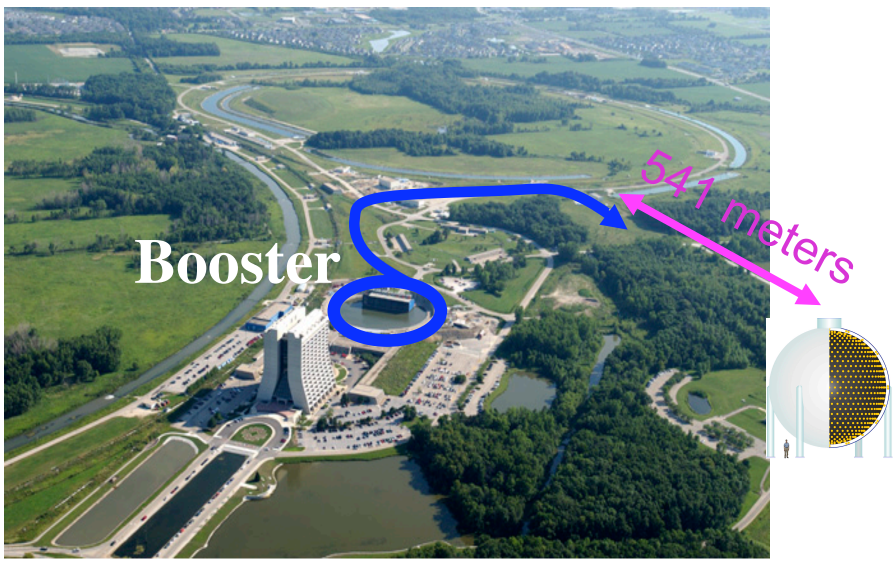

The MiniBooNE Detector

- 541 meters downstream of target
- 3 meter overburden
- 12 meter diameter sphere

  (10 meter “fiducial” volume)
- Filled with 800 t of pure mineral oil (CH_2)

  (Fiducial volume: 450 t)
- 1280 inner phototubes,
- 240 veto phototubes

  Simulated with a GEANT3 Monte Carlo

MiniBooNE collaboration,
NIM.A599(2009)28

2. MiniBooNE detector

The MiniBooNE Detector

- 541 meters downstream of target
- 3 meter overburden
- 12 meter diameter sphere

  (10 meter “fiducial” volume)
- Filled with 800 t of pure mineral oil (CH_2)

  (Fiducial volume: 450 t)
- 1280 inner phototubes,
- 240 veto phototubes

  Simulated with a GEANT3 Monte Carlo

MiniBooNE collaboration,
NIM.A599(2009)28

2. MiniBooNE detector

The MiniBooNE Detector

- 541 meters downstream of target
- 3 meter overburden
- 12 meter diameter sphere

  (10 meter “fiducial” volume)
- Filled with 800 t of pure mineral oil (CH_2)

  (Fiducial volume: 450 t)
- 1280 inner phototubes,
- 240 veto phototubes

  Simulated with a GEANT3 Monte Carlo

MiniBooNE collaboration,
NIM.A599(2009)28

2. MiniBooNE detector

The MiniBooNE Detector

- 541 meters downstream of target
- 3 meter overburden
- 12 meter diameter sphere

  (10 meter “fiducial” volume)
- Filled with 800 t of pure mineral oil (CH_2)

  (Fiducial volume: 450 t)
- 1280 inner phototubes,
- 240 veto phototubes

  Simulated with a GEANT3 Monte Carlo

MiniBooNE collaboration, NIM.A599(2009)28

2. Events in the detector

- ***Muons***
  - ***Sharp, clear rings***
    - ***Long, straight tracks***
- Electrons
  - Scattered rings
    - Multiple scattering
    - Radiative processes

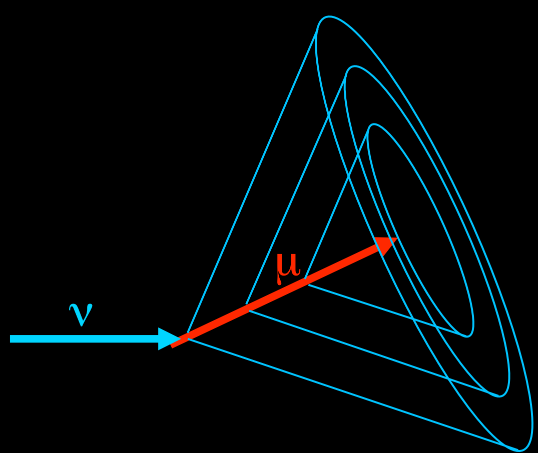

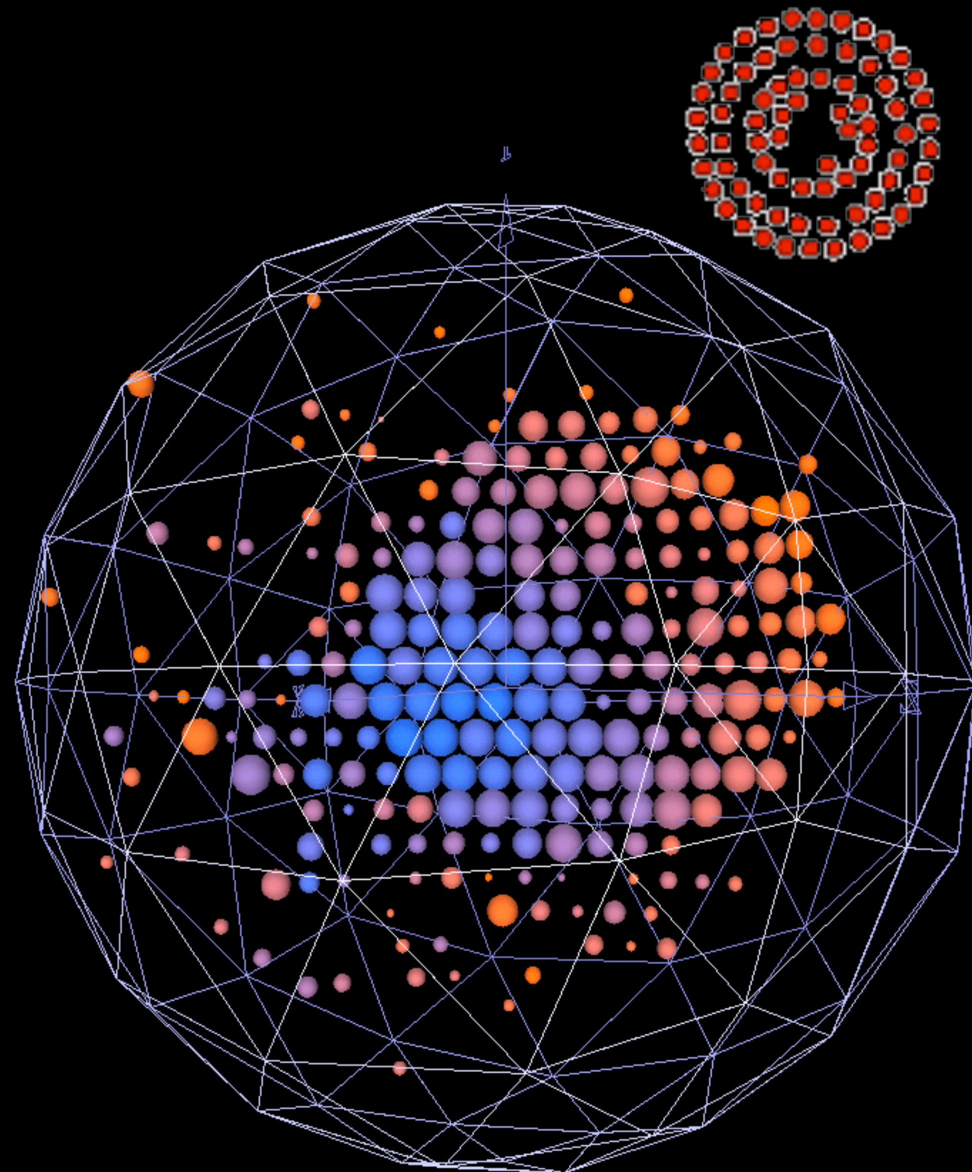

MiniBooNE collaboration,
NIM.A599(2009)28

2. Events in the detector

- Muons
  - Sharp, clear rings
    - Long, straight tracks
- ***Electrons***
  - ***Scattered rings***
    - ***Multiple scattering***
    - ***Radiative processes***

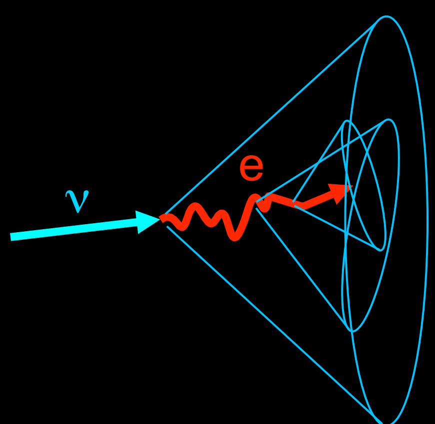

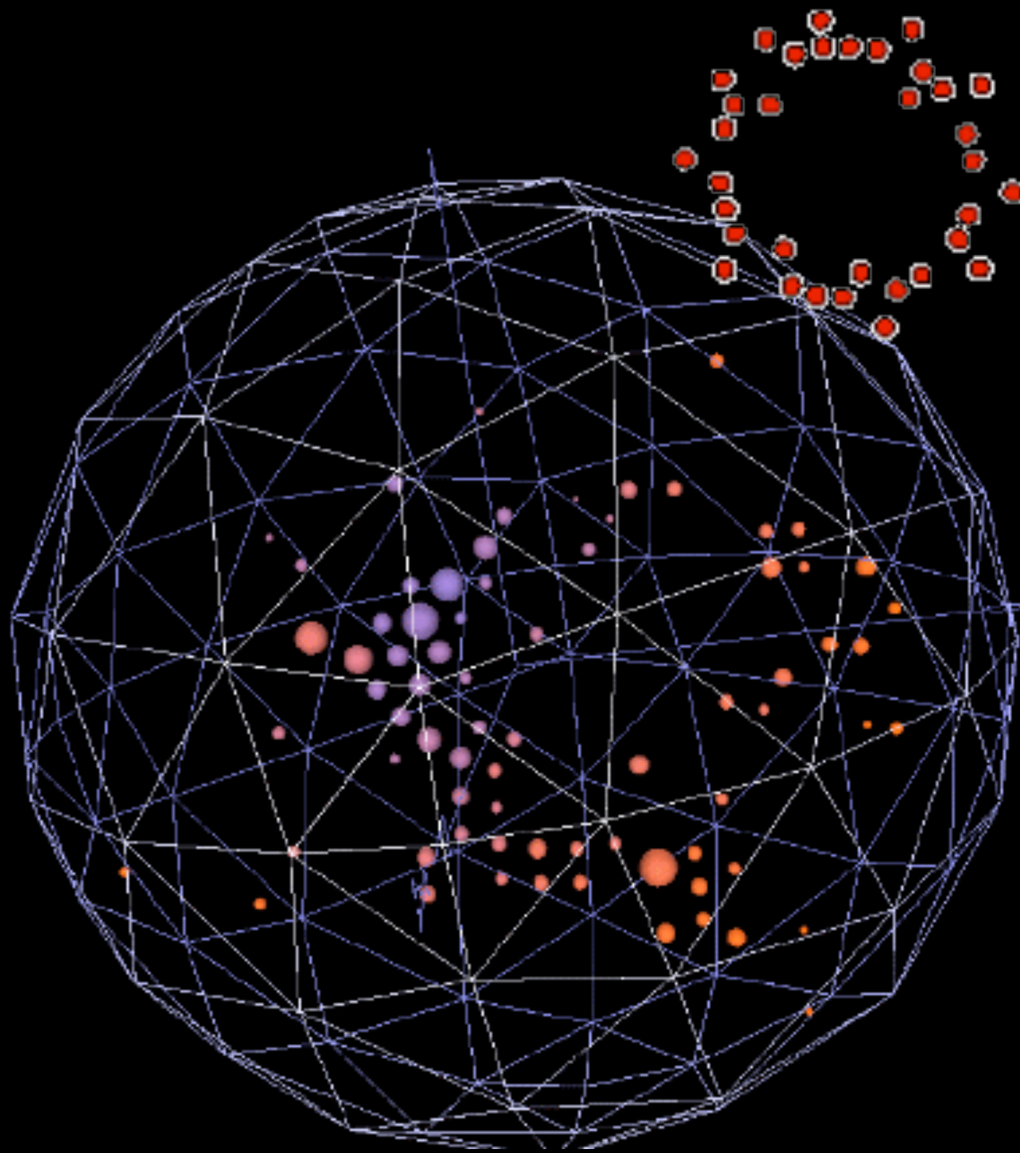

1. Booster neutrino beamline

2. MiniBooNE detector

3. CCQE events in MiniBooNE

4. CC1π background constraint

5. CCQE M_A^{eff}-κ shape-only fit

6. CCQE absolute cross section

7 Conclusion

3. CCQE event measurement in MiniBooNE

ν_μ charged current quasi-elastic (ν_μ CCQE) interaction is an important channel for the neutrino oscillation physics and the most abundant (~40%) interaction type in MiniBooNE detector

$$\nu_\mu + n \to p + \mu^-$$

$$(\nu_\mu + {}^{12}C \to X + \mu^-)$$

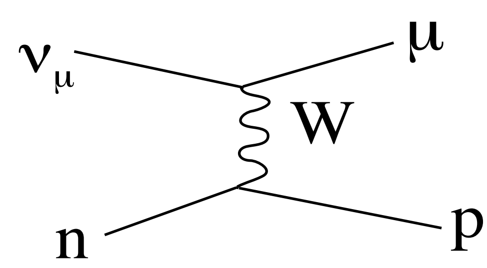

MiniBooNE detector

(spherical Cherenkov detector)

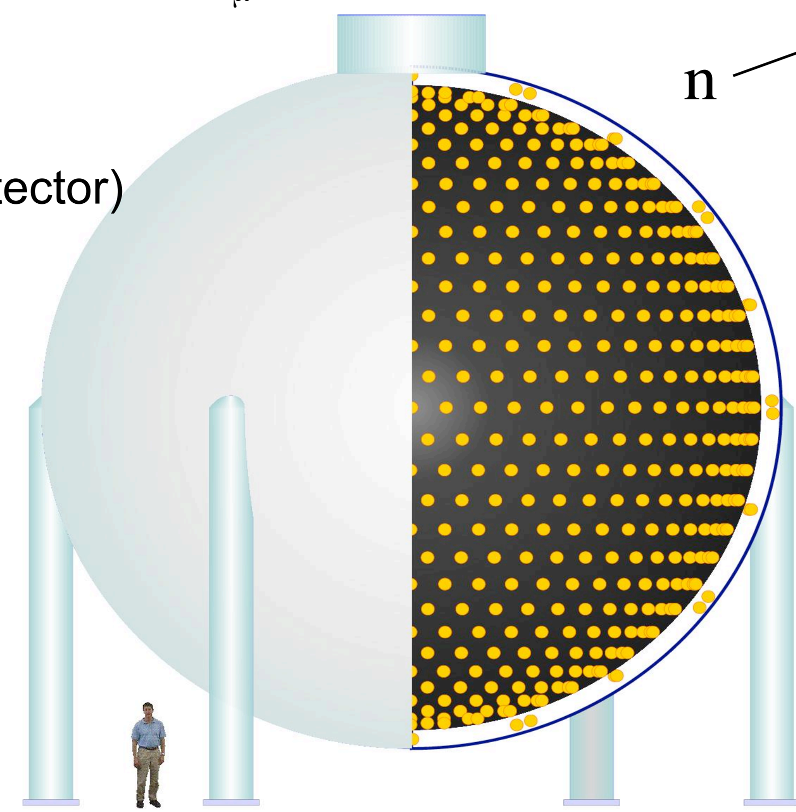

3. CCQE event measurement in MiniBooNE

ν_μ charged current quasi-elastic (ν_μ CCQE) interaction is an important channel for the neutrino oscillation physics and the most abundant (~40%) interaction type in MiniBooNE detector

$$\nu_\mu + n \rightarrow p + \mu^-$$

$$(\nu_\mu + {}^{12}C \rightarrow X + \mu^-)$$

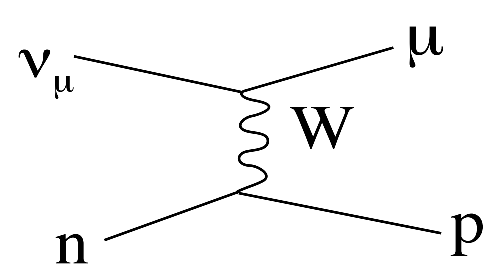

MiniBooNE detector
(spherical Cherenkov detector)

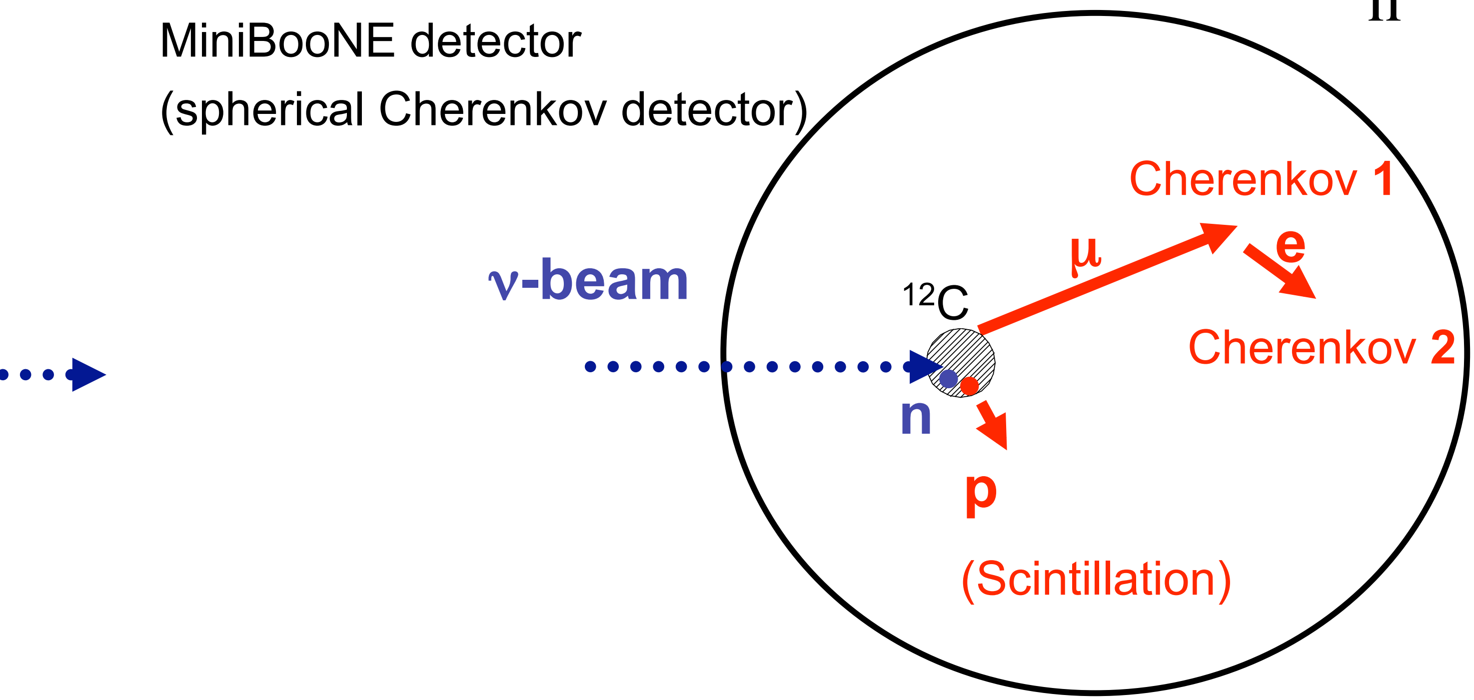

muon like Cherenkov light and subsequent decayed electron (Michel electron) like Cherenkov light are the signal of CCQE event

3. CCQE event measurement in MiniBooNE

ν_μ CCQE interactions (ν+n $\rightarrow$ μ+p) has characteristic two “subevent” structure from muon decay

$$\nu_\mu + n \rightarrow \overset{1}{\boxed{\mu^-}} + p \rightarrow \nu_\mu + \overline{\nu_e} + \overset{2}{\boxed{e^-}} + p$$

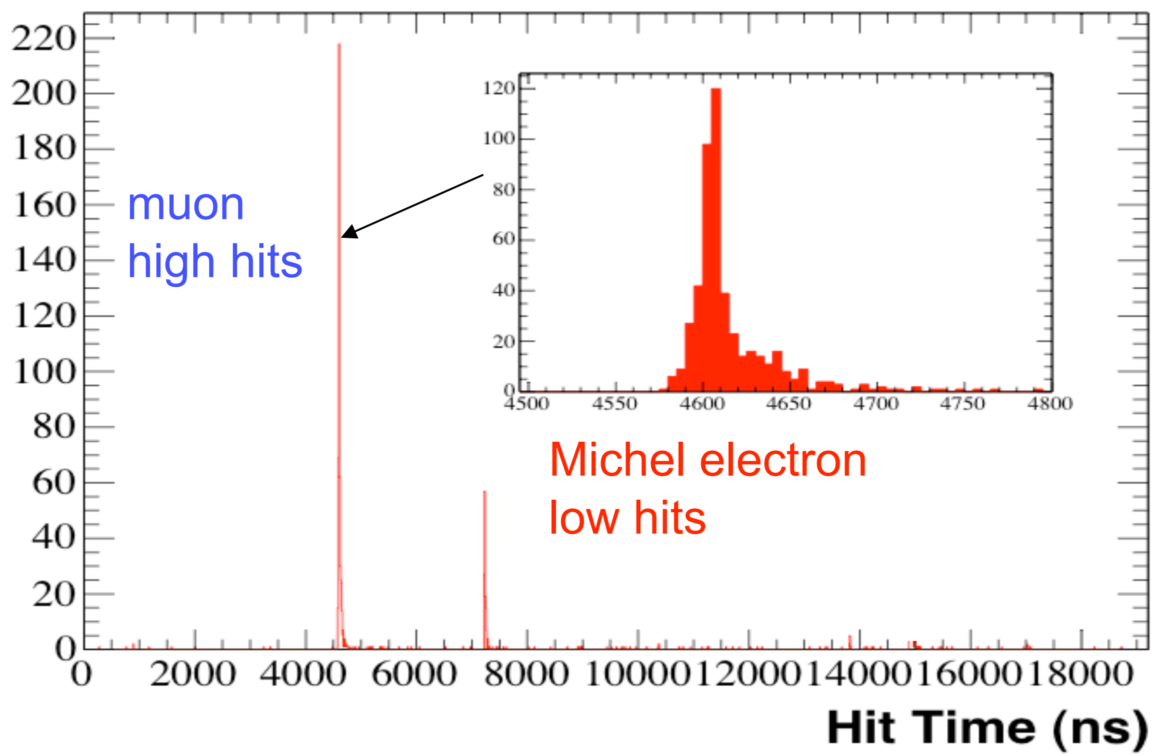

27% efficiency
77% purity
146,070 events
with 5.58E20POT

3. CCQE event measurement in MiniBooNE

All kinematics are specified from 2 observables, muon energy E_μ and muon scattering angle θ_μ

Energy of the neutrino E_ν^{QE} and 4-momentum transfer Q^2_{QE} can be reconstructed by these 2 observables, under the assumption of CCQE interaction with bound neutron at rest ("QE assumption")

$$E_\nu^{QE} = \frac{2(M-E_B)E_\mu - (E_B^2 - 2ME_B + m_\mu^2 + \Delta M^2)}{2[(M-E_B) - E_\mu + p_\mu \cos\theta_\mu]}$$

$$Q_{QE}^2 = -m_\mu^2 + 2E_\nu^{QE}(E_\mu - p_\mu \cos\theta_\mu)$$

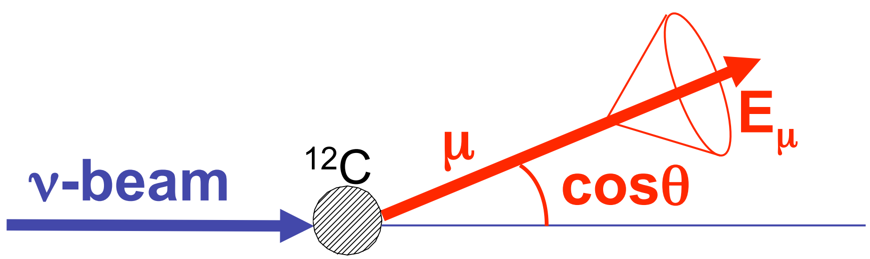

1. Booster neutrino beamline

2. MiniBooNE detector

3. CCQE events in MiniBooNE

4. CC1π background constraint

5. CCQE M_A^{eff}-κ shape-only fit

6. CCQE absolute cross section

7 Conclusion

4. CC1π background constraint, introduction

data-MC comparison, in 2 subevent sample (absolute scale)

CCQE sample shows good agreement in shape, because we tuned relativistic Fermi gas (RFG) parameters.

MiniBooNE collaboration, PRL100(2008)032301

CCQE

$$\nu_\mu + n \to \overset{1}{\boxed{\mu^-}} + p \to \nu_\mu + \overline{\nu}_e + \overset{2}{\boxed{e^-}} + p$$

However absolute normalization does not agree.

CC1π

$$\nu_\mu + N \to \overset{1}{\boxed{\mu^-}} + \cancel{\pi^+} + N \to \nu_\mu + \overline{\nu}_e + \overset{2}{\boxed{e^-}} + N$$

(π-absorption)

The background is dominated with CC1π without pion (CCQE-like). We need a background prediction with an absolute scale.

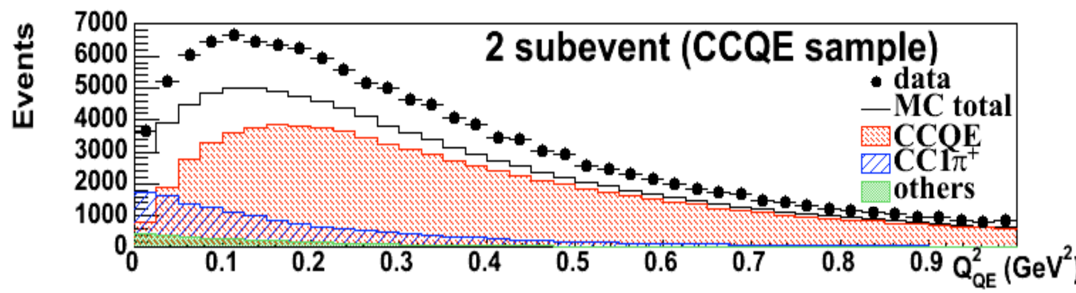

4. CC1π background constraint, introduction

data-MC comparison, in 3 subevent sample (absolute scale)

CCQE-CC1π simultaneous measurement is performed.

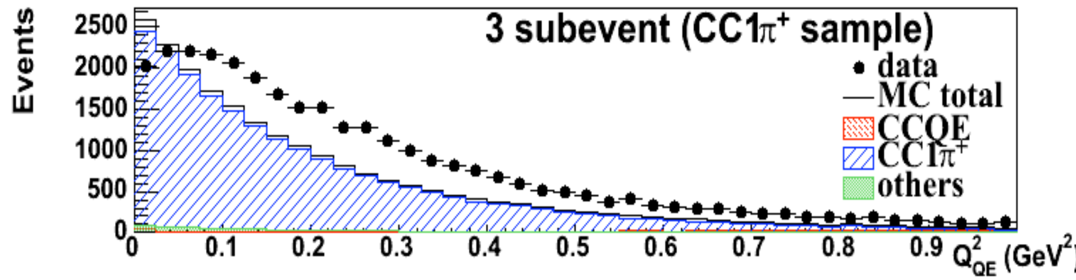

CC1π

$$\nu_\mu + N \rightarrow \overset{1}{\boxed{\mu^-}} + \pi^+ + N \rightarrow \nu_\mu + \overline{\nu}_e + \overset{2}{\boxed{e^-}} + N$$

$$\pi^+ \rightarrow \nu_\mu + \mu^+ \rightarrow \nu_\mu + \overline{\nu}_e + \overset{3}{\boxed{e^+}} + N$$

4. CC1π background constraint

data-MC comparison, before CC1π constraint (absolute scale)

CCQE-CC1π simultaneous measurement is performed.

We use data-MC Q^2 ratio in CC1π sample to correct all CC1π events in MC.

Then, this "new" MC is used to predicts CC1π background in CCQE sample

This correction gives both CC1π background normalization and shape in CCQE sample

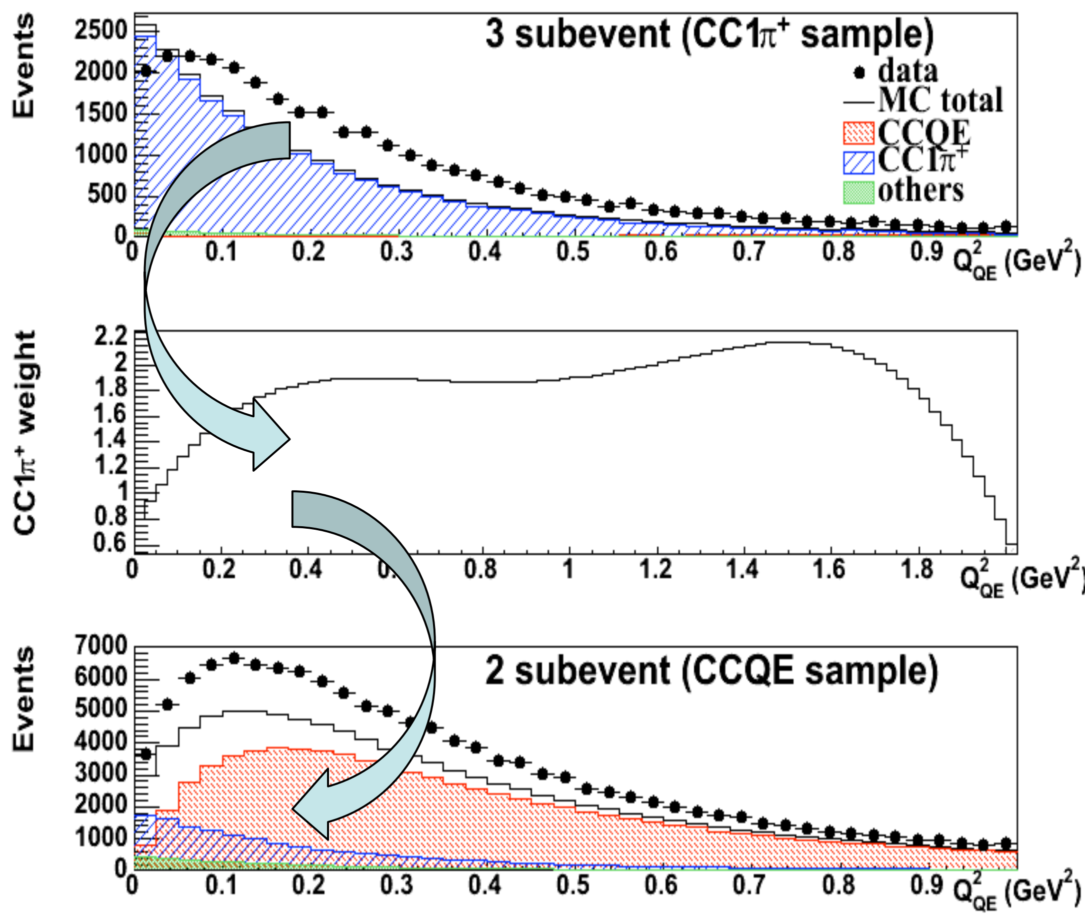

4. CC1π background constraint

data-MC comparison, after CC1π constraint (absolute scale)

Now we have an absolute prediction of CC1π background in CCQE sample.

We are ready to measure the absolute CCQE cross section!

Precise background prediction is essential for precise cross section measurement

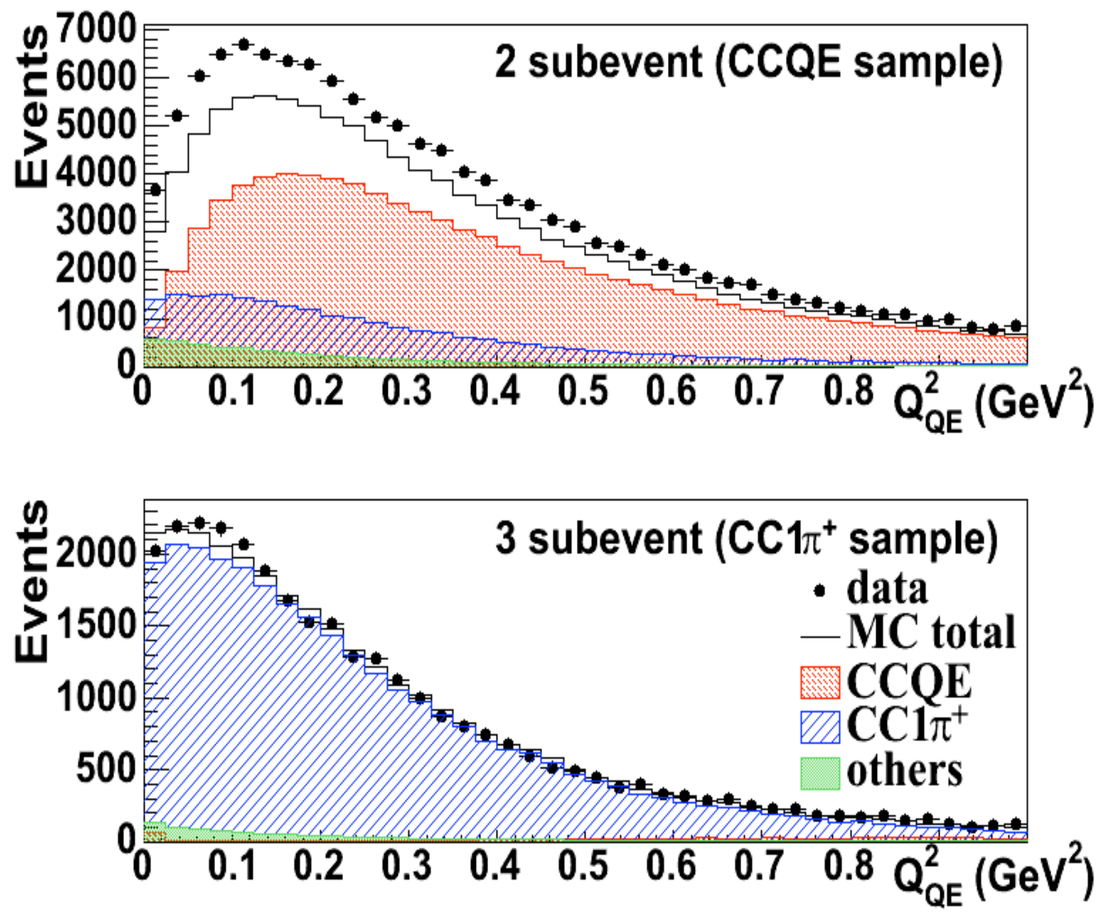

1. Booster neutrino beamline

2. MiniBooNE detector

3. CCQE events in MiniBooNE

4. CC1π background constraint

5. CCQE M_A^{eff}-κ shape-only fit

6. CCQE absolute cross section

7 Conclusion

Smith and Moniz,
Nucl.,Phys.,B43(1972)605

5. Relativistic Fermi Gas (RFG) model

Relativistic Fermi Gas (RFG) Model

Carbon is described by the collection of incoherent Fermi gas particles.
All details come from hadronic tensor.

$$(W_{\mu\nu})_{ab} = \int_{Elo}^{Ehi} f(\vec{k},\vec{q},w) T_{\mu\nu} dE \text{ : hadronic tensor}$$

$$f(\vec{k},\vec{q},w) \text{ : nucleon phase space density function}$$

$$T_{\mu\nu} = T_{\mu\nu}(F_1, F_2, F_A, F_P) \text{ : nucleon tensor}$$

$$F_A(Q^2) = g_A/(1+Q^2/\boxed{M_A^2})^2 \text{ : Axial form factor}$$

$$Ehi \text{ : the highest energy state of nucleon } = \sqrt{(p_F^2 + M^2)}$$

$$Elo \text{ : the lowest energy state of nucleon } = \boxed{\kappa}\left(\sqrt{(p_F^2 + M^2)} - \omega + E_B\right)$$

We tuned following 2 parameters using Q^2 distribution by least χ^2 fit;

M_A = effective axial mass

κ = Pauli blocking parameter

5. M_A^{eff}-κ shape-only fit

κ goes down and M_A goes up from previous study, due to the shape change of the background. Now κ is consistent with 1.

M_A^{eff} - κ shape-only fit result

M_A^{eff} = 1.35 ± 0.17 GeV (stat+sys)
κ = 1.007 ± 0.12 (stat+sys)
χ^2/ndf = 47.0/38

Q2 fits to MB ν_μ CCQE data using the nuclear parameters:

$M_A$eff - effective axial mass
κ - Pauli Blocking parameter

Relativistic Fermi Gas Model with tuned parameters describes ν_μ CCQE data well

Q2 distribution before and after fitting

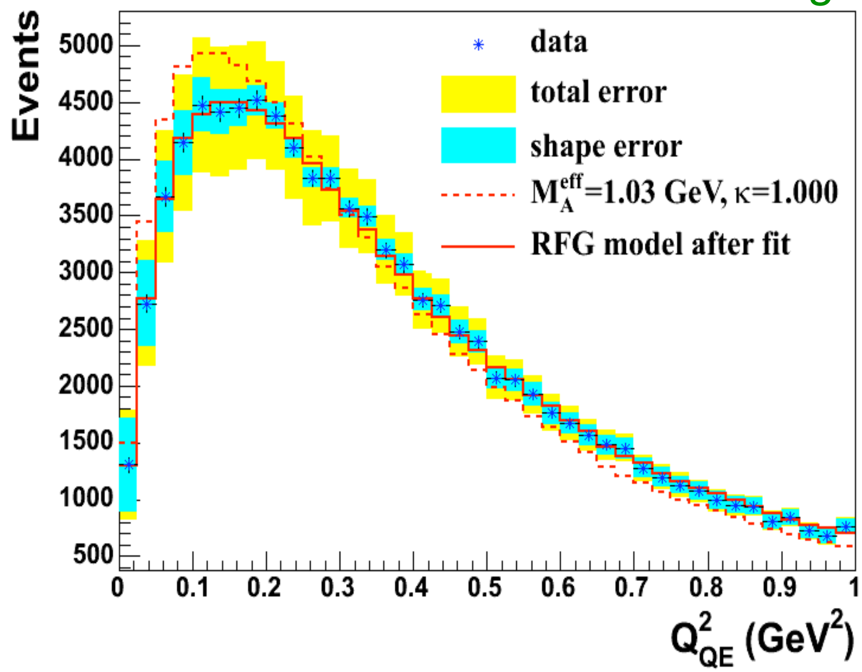

5. M_A^{eff}-κ shape-only fit

Caution!
This new CCQE model doesn't affect our cross section result

M_A^{eff} - κ shape-only fit result

M_A^{eff} = 1.35 ± 0.17 GeV (stat+sys)
κ = 1.007 ± 0.12 (stat+sys)
χ^2/ndf = 47.0/38

Data-MC agreement in T_μ-cosθ kinematic plane is good.

World averaged RFG model
M_A^{eff} = 1.03, κ = 1.000

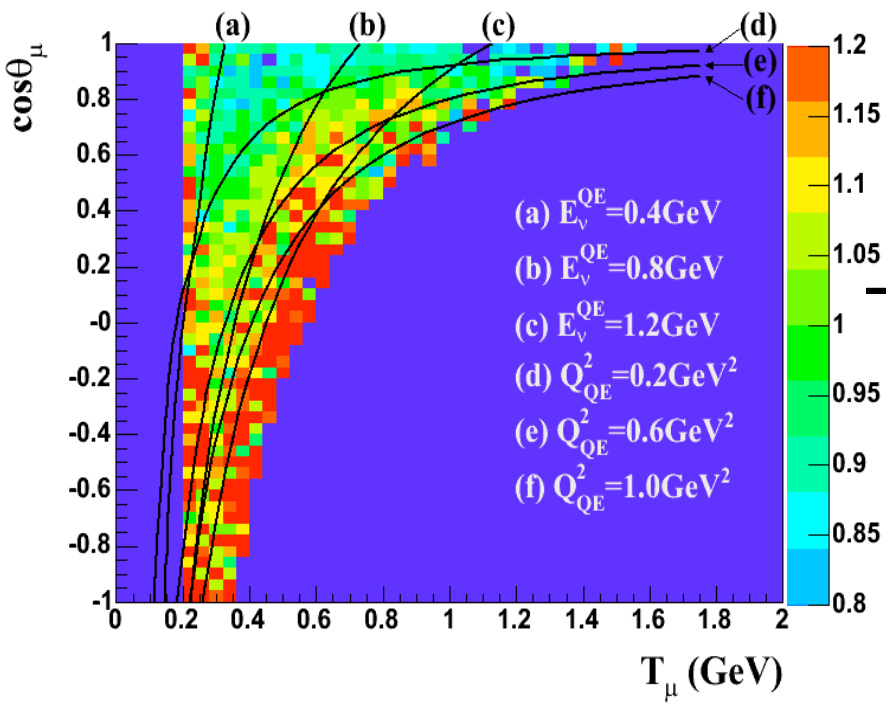

data-MC ratio in T_μ-cosθ kinematic plane after fit

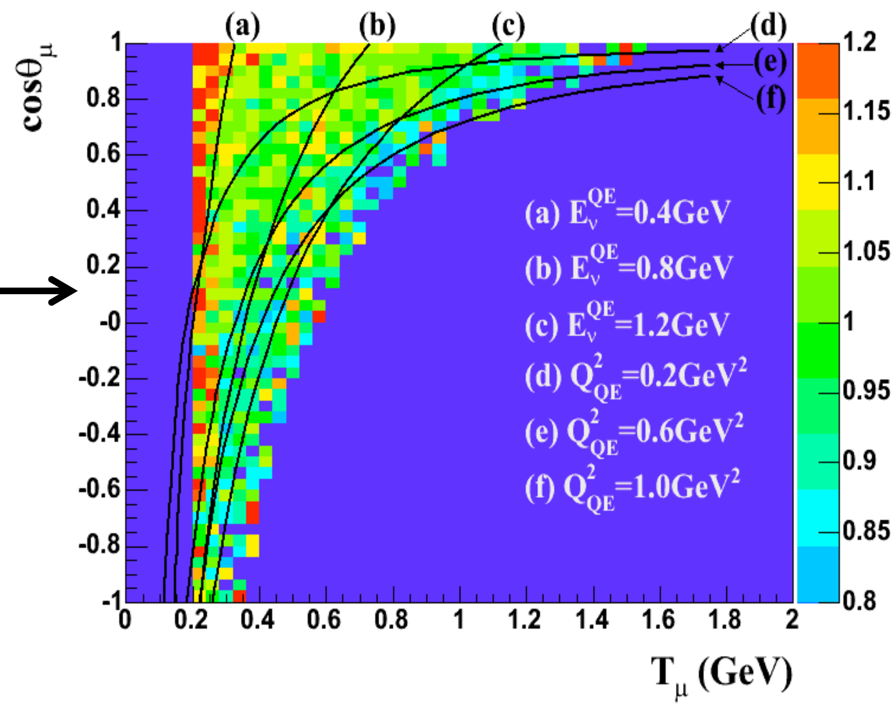

MiniBooNE collaboration,
PRL100(2008)032301

5. T_μ-$\cos\theta_\mu$ plane

Without knowing flux perfectly, we cannot modify cross section model

$$R(\mathrm{interaction}) \propto \int (\mathrm{flux}) \times (\mathrm{xs})$$

Data-MC ratio for T_μ-$\cos\theta_\mu$ plane, before tuning

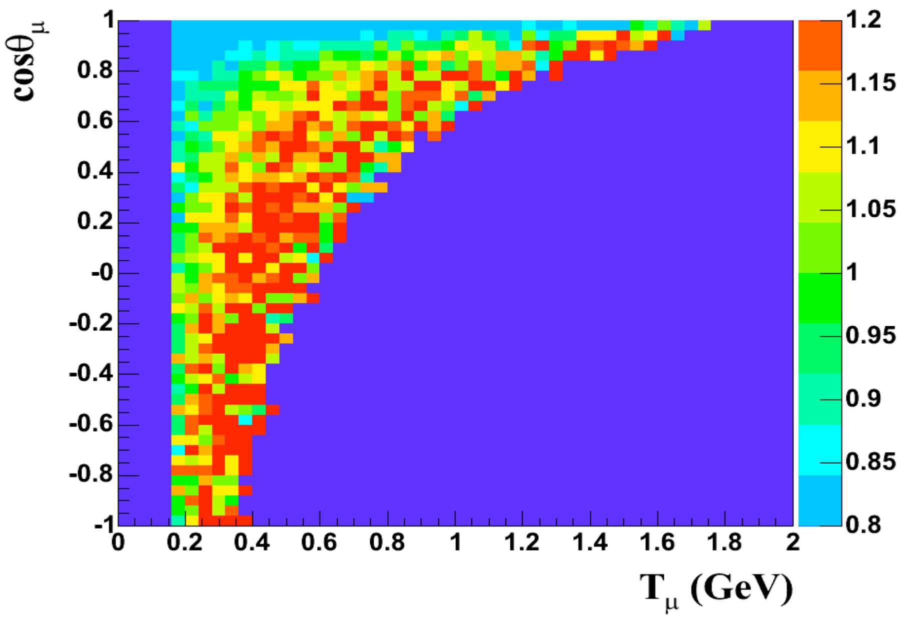

MiniBooNE collaboration, PRL100(2008)032301

5. T_μ-$\cos\theta_\mu$ plane

Without knowing flux perfectly, we cannot modify cross section model

$$R(\text{interaction}[E_\nu, Q^2]) \propto \int (\text{flux}[E_\nu]) \times (\text{xs}[Q^2])$$

Data-MC mismatching follows Q2 lines, not E_ν lines, therefore we can see the problem is not the flux prediction, but the cross section model

Data-MC ratio for T_μ-$\cos\theta_\mu$ plane, before tuning

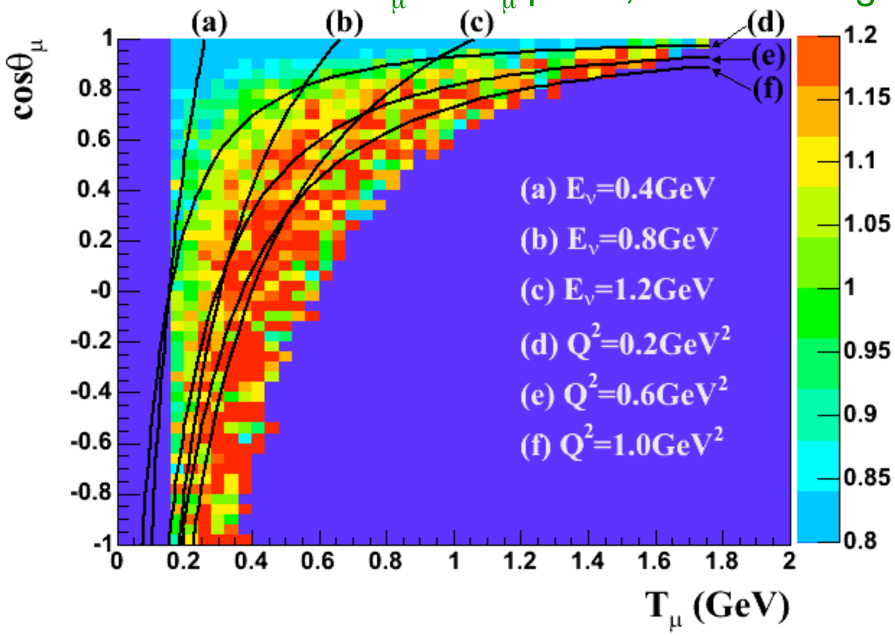

5. T_μ-$\cos\theta_\mu$ plane

MiniBooNE collaboration,
PRL100(2008)032301

Without knowing flux perfectly, we cannot modify cross section model

$$R(\mathrm{interaction}[E_\nu, Q^2]) \propto \int (\mathrm{flux}[E_\nu]) \times (\mathrm{xs}[Q^2])$$

Data-MC mismatching follows Q2 lines, not E_ν lines, therefore we can see the problem is not the flux prediction, but the cross section model

Data-MC ratio for T_μ-$\cos\theta_\mu$ plane, before tuning

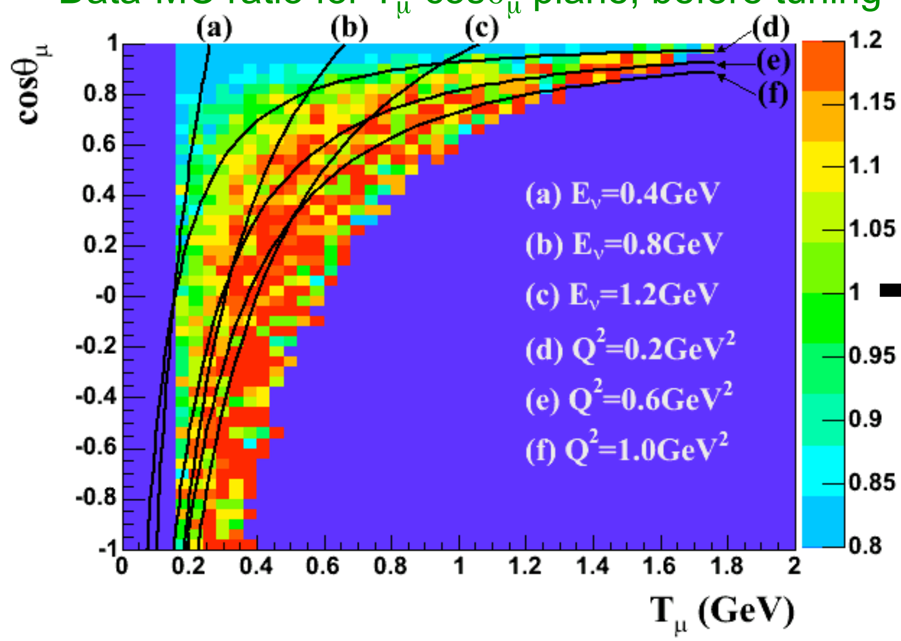

Data-MC ratio for T_μ-$\cos\theta_\mu$ plane,after tuning

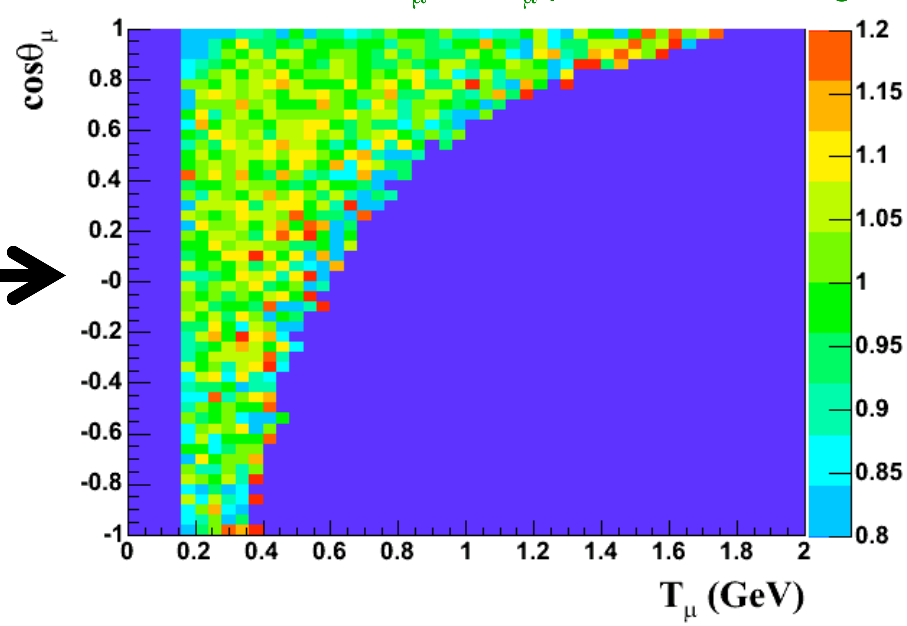

1. Booster neutrino beamline

2. MiniBooNE detector

3. CCQE events in MiniBooNE

4. CC1π background constraint

5. CCQE M_A^{eff}-κ shape-only fit

6. CCQE absolute cross section

7 Conclusion

6. CCQE absolute cross section

Flux-integrated single differential cross section (Q^2_{QE})

The data is compared with various RFG model with neutrino flux averaged.

Compared to the world averaged CCQE model (red), our CCQE data is 30% high.

Our model extracted from shape-only fit has better agreement with (within our total normalization error).

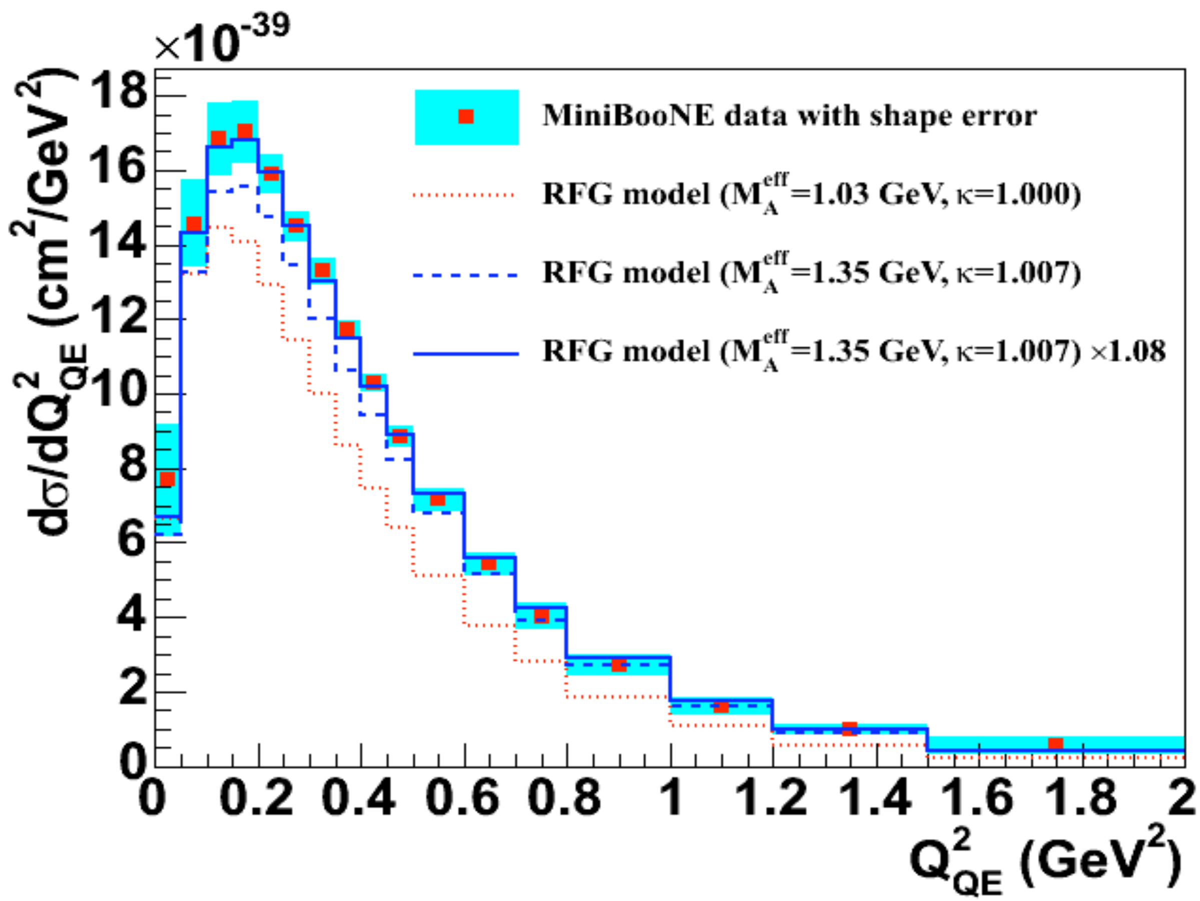

6. CCQE-like absolute cross section

Flux-integrated single differential cross section (Q^2_{QE})

Irreducible background distribution is overlaid.

Sum of CCQE cross section and irreducible background makes cross section of CCQE-like sample.

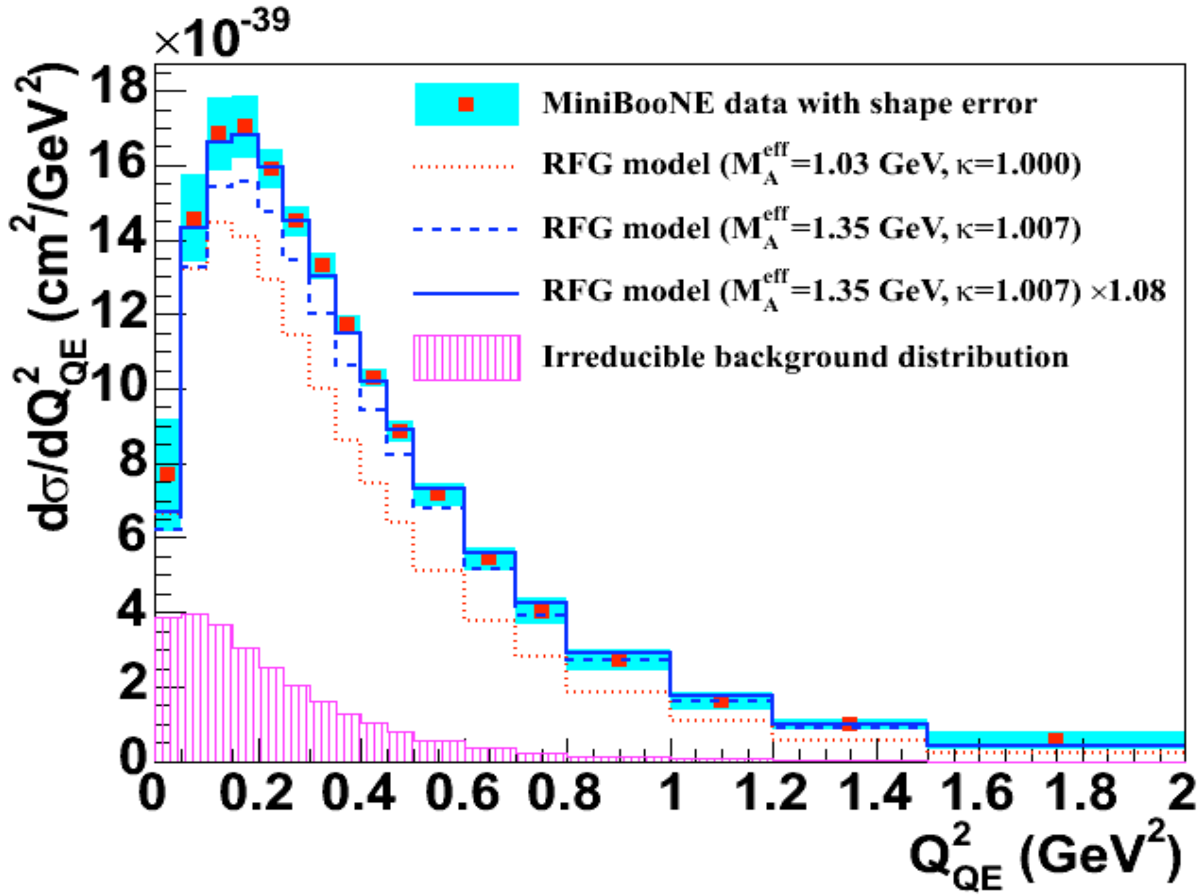

6. CCQE absolute cross section

Flux-unfolded total cross section ($E_\nu^{QE,RFG}$)

New CCQE model is tuned from shape-only fit in Q^2, and it also describes normalization well.

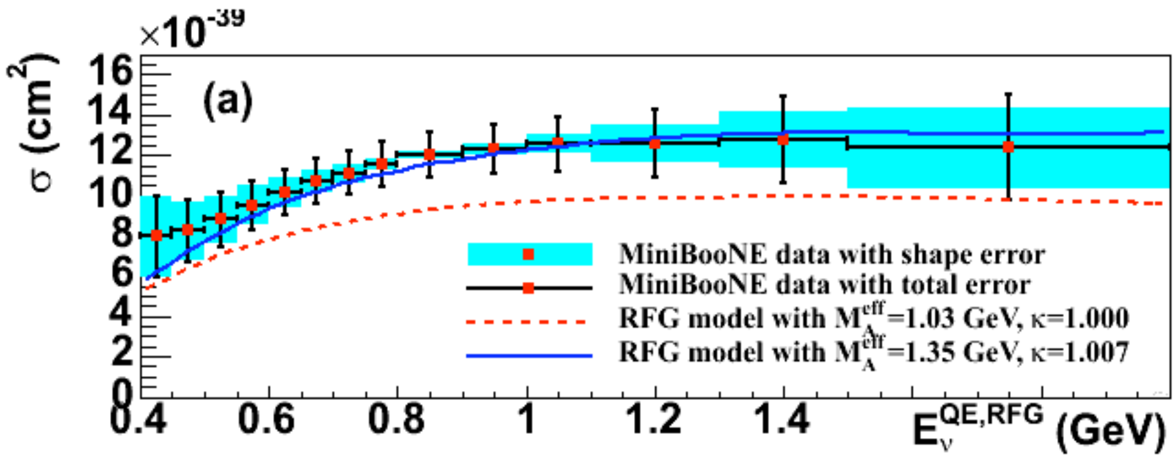

6. CCQE errors

Error summary (systematic error dominant)

Flux error dominates the total normalization error.

Cross section error is small because of high purity and in situ background measurement.

Detector error dominates shape error, because this is related with energy scale.

Unfolding error is the systematic error associated to unfolding (iterative Bayesian method).

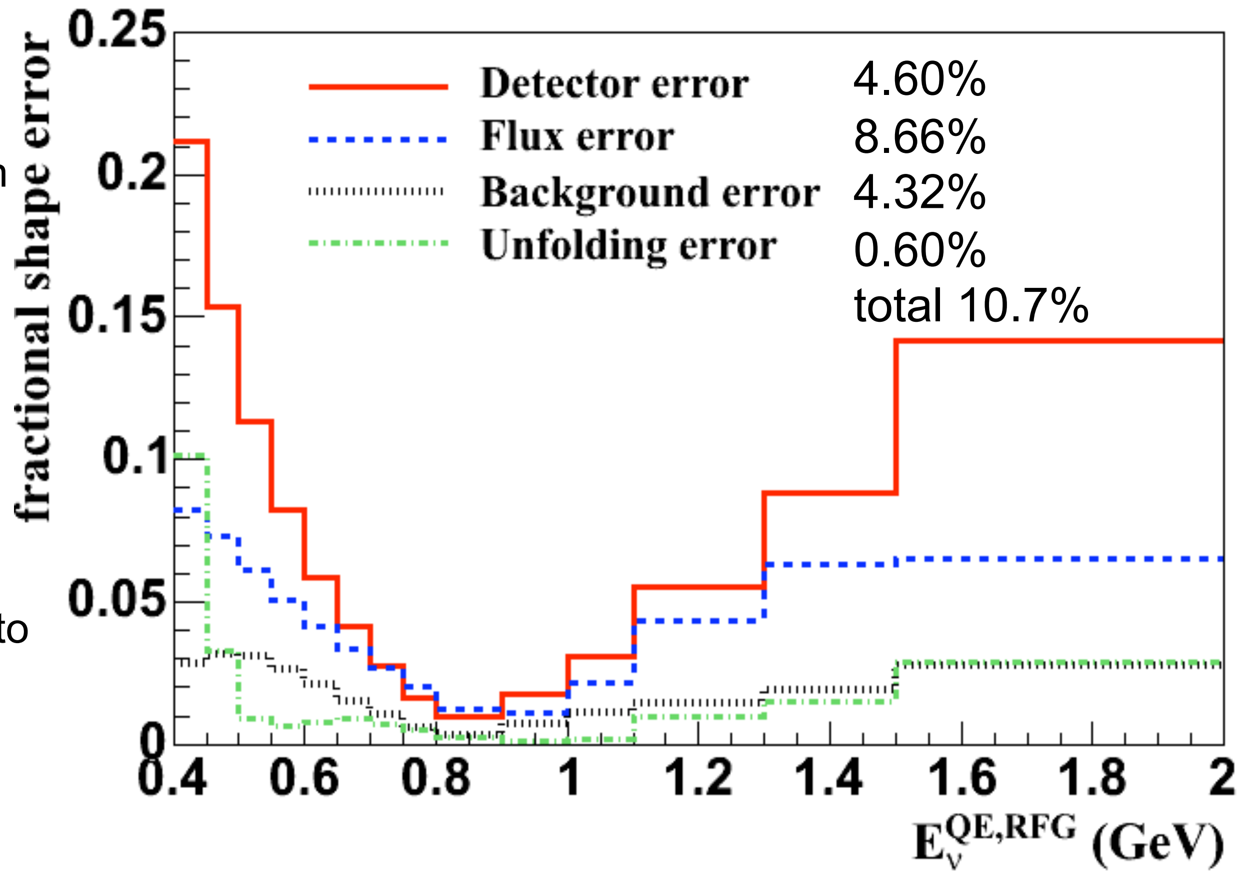

NOMAD collaboration, Eur.Phys.J.C63(2009)355

6. QE cross section comparison with NOMAD

Flux-unfolded total cross section ($E_\nu^{QE,RFG}$)

New CCQE model is tuned from shape-only fit in Q^2, and it also describes normalization well.

Comparing with NOMAD, MiniBooNE cross section is 30% higher, but these 2 experiments leave a gap in energy to allow some interesting physics.

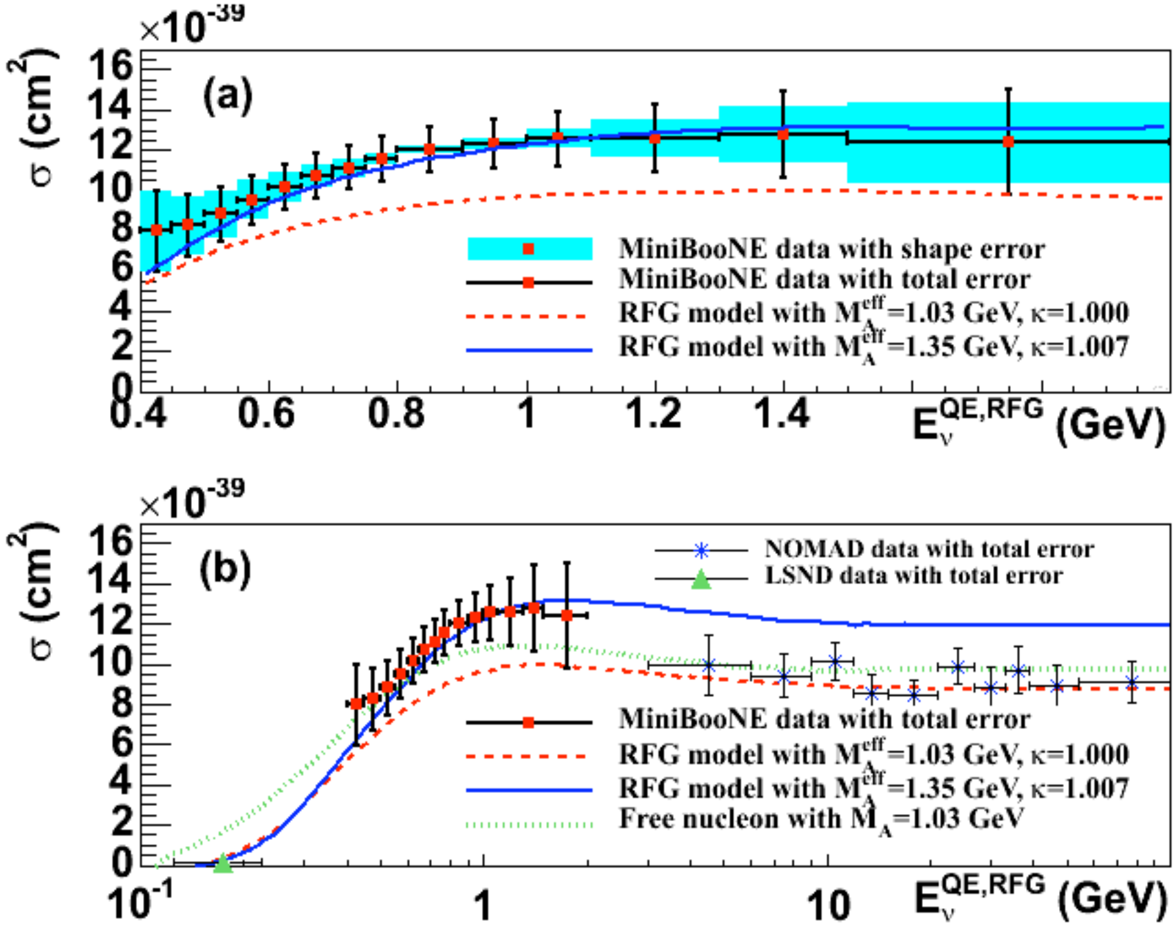

NOMAD collaboration,
Eur.Phys.J.C63(2009)355

6. CCQE total cross section model dependence

Flux-unfolded total cross section ($E_\nu^{QE,RFG}$)

Unfortunately, flux-unfolded cross section is model dependent.

Reconstruction bias due to "QE" assumption is corrected under "RFG" model assumption.

One should be careful when comparing flux-unfolded data from different experiments.

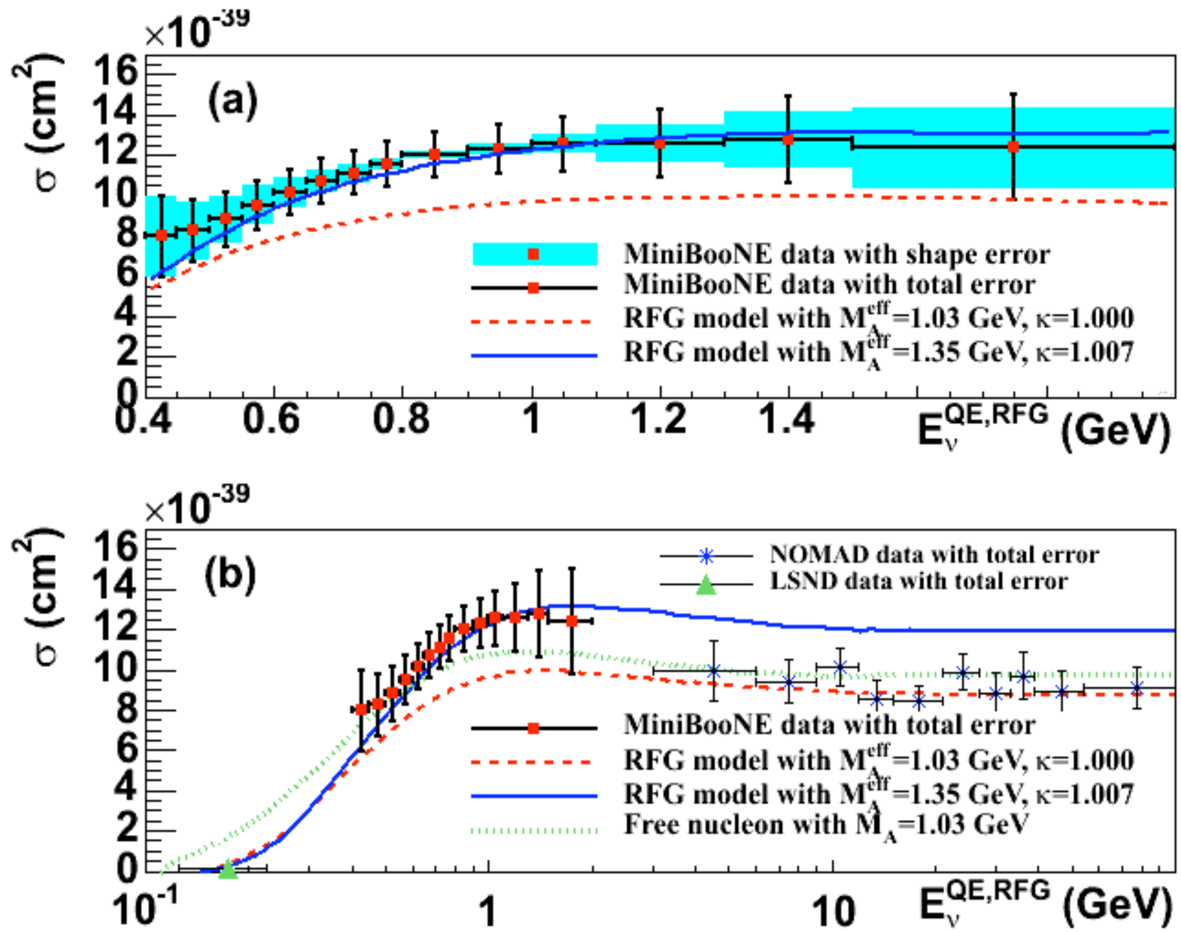

6. CCQE total cross section model dependence

Flux-unfolded total cross section (E_ν^{RFG})

Unfortunately, flux-unfolded cross section is model dependent.

Reconstruction bias due to "QE" assumption is corrected under "RFG" model assumption.

One should be careful when comparing flux-unfolded data from different experiments.

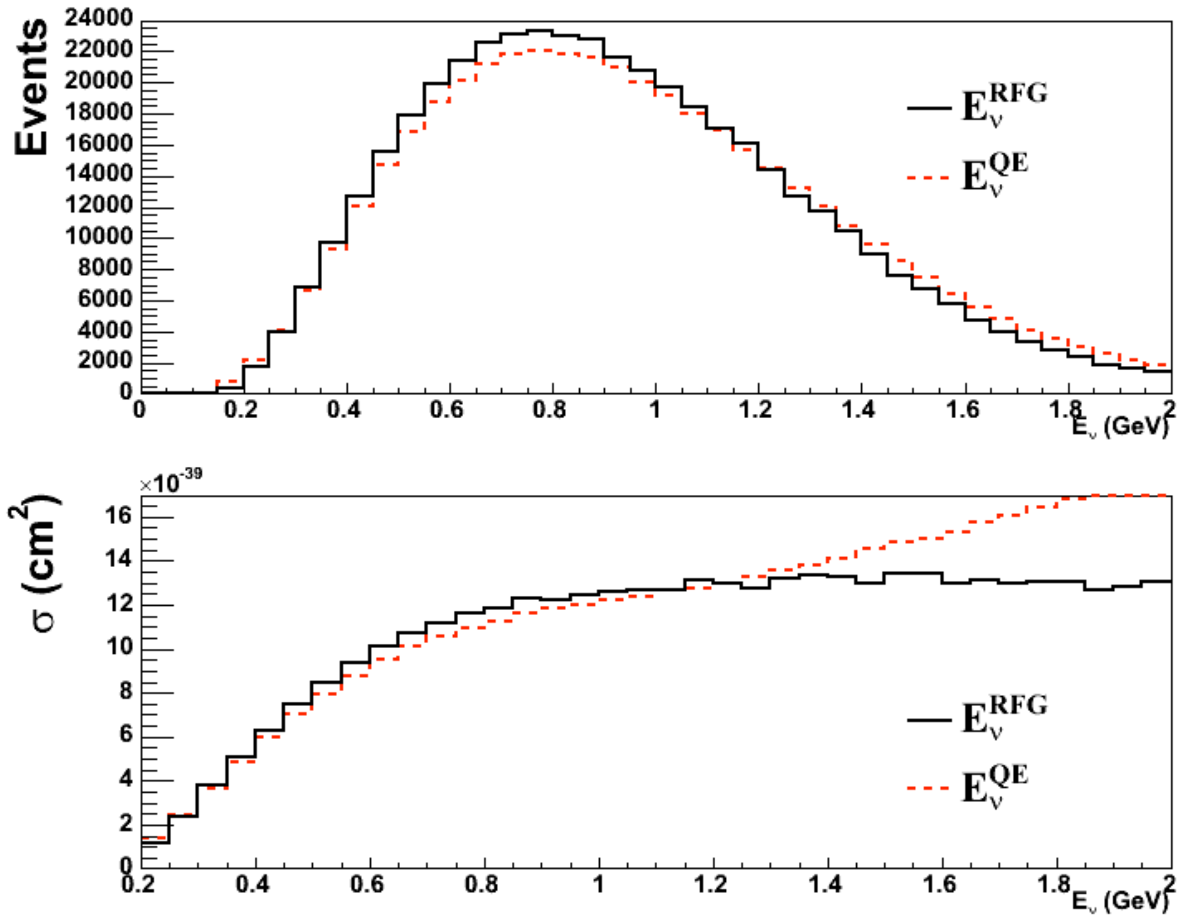

6. CCQE double differential cross section

Flux-integrated double differential cross section (T_μ-$\cos\theta$)

This is the most complete information about neutrino cross section based on muon kinematic measurement.

The error shown here is shape error, a total normalization error (δN_T=10.7%) is separated.

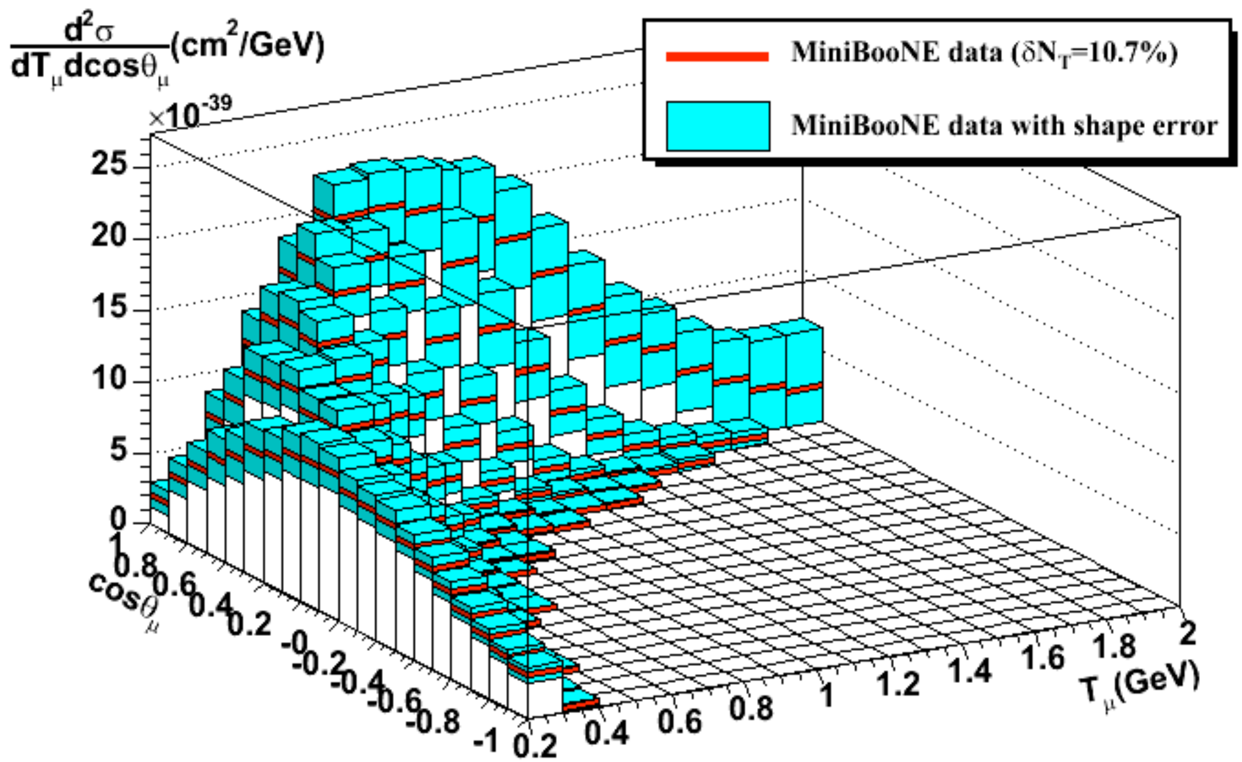

6. Paradigm shift in neutrino cross section!?

Theoretical approaches for the large cross section and harder Q^2 spectrum

RPA formalism Martini et al.,PRC80(2009)065501

SRC+MEC Carlson et al.,PRC65(2002)024002

The presence of a polarization cloud (tensor interaction) surrounding a nucleon in the nuclear medium contribute large 2p-2h interaction. Since MiniBooNE counts multi nucleon emission as CCQE, 2p-2h interaction is counted as CCQE and it enhances CCQE more than 40%.

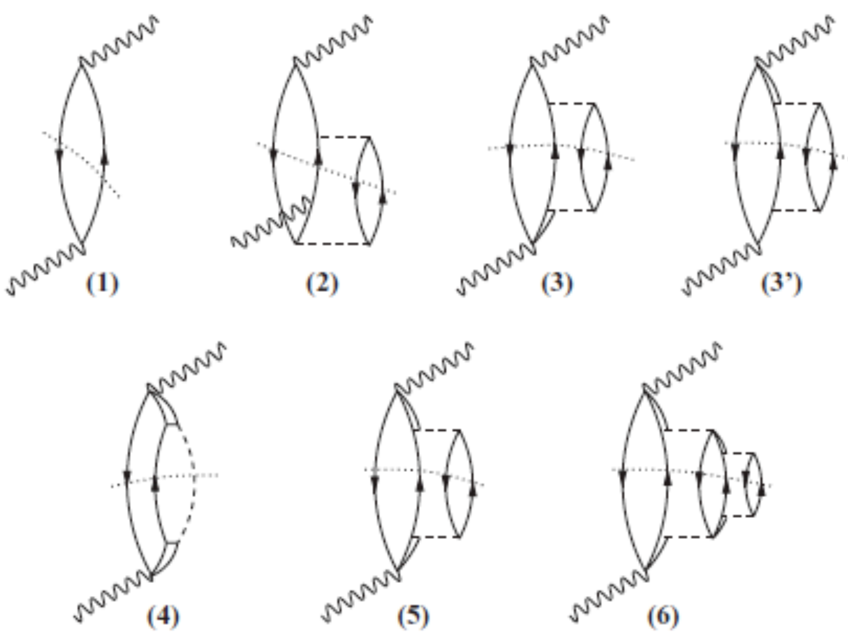

FIG. 1. Feynman graphs of the partial polarization propagators:

QE+np-nh and MiniBooNE data

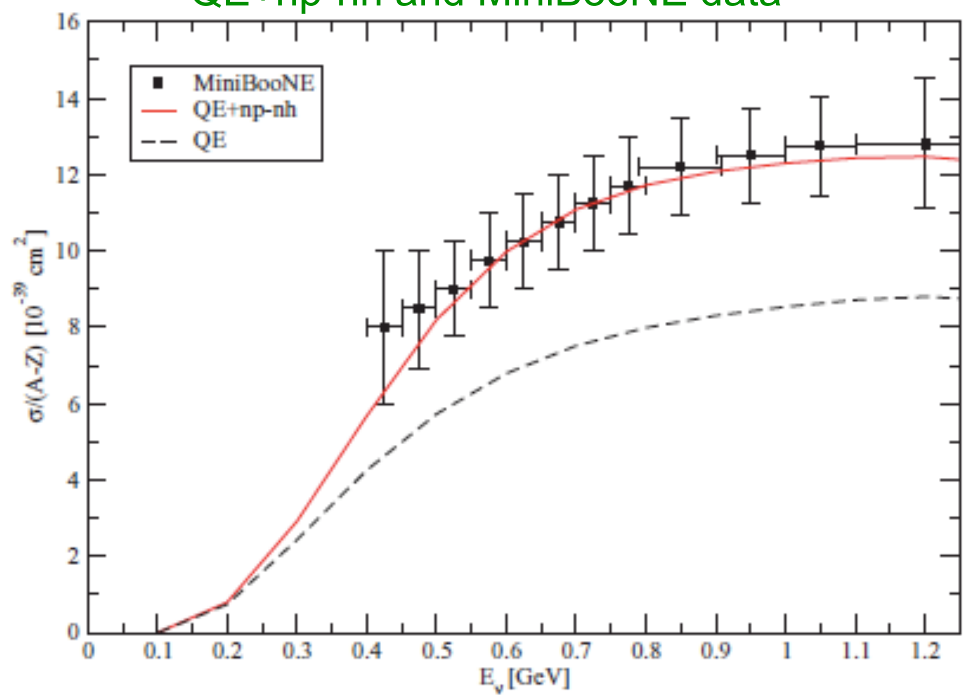

6. Paradigm shift in neutrino cross section!?

Theoretical approaches for the large cross section and harder Q^2 spectrum

RPA formalism Martini et al.,PRC80(2009)065501

SRC+MEC Carlson et al.,PRC65(2002)024002

Transverse response is enhanced by presence of short range correlation (SRC) and 2-body current (meson exchange current, MEC).

Euclidian response of e-^{4}He (|q|=600MeV/c)

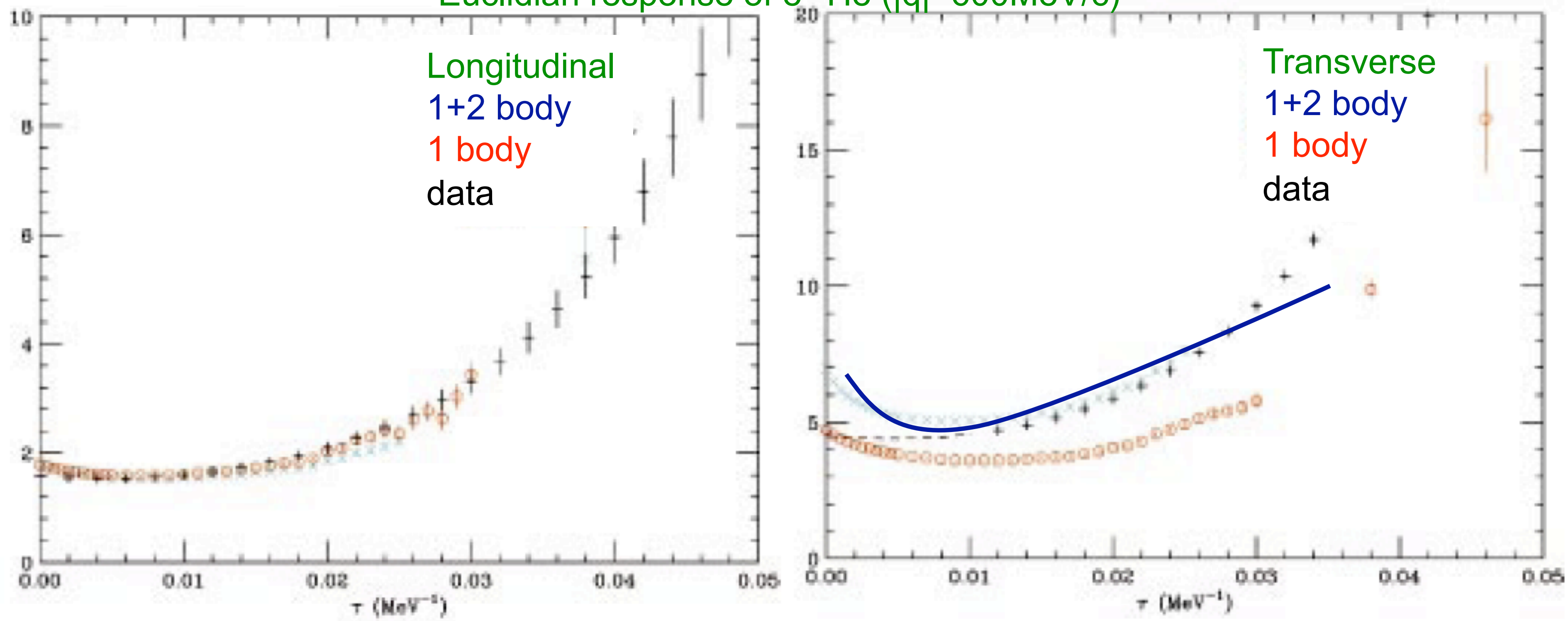

7. Conclusions

Using the high statistics and high purity MiniBooNE ν_μ CCQE data sample (146,070 events, 27% efficiency, and 77% purity), the absolute cross section is measured. We especially emphasize the measurement of flux-integrated double differential cross section, because this is the most complete set of information for muon kinematics based neutrino interaction measurement. The double differential cross section is the model independent result.

We measured 30% higher cross section than RFG model with the world averaged nuclear parameter. Interesting to note, our total cross section is consistent with RFG model with nuclear parameters extracted from shape-only fit in our Q^2 data.

7. Conclusions

Realizations from MiniBooNE CCQE analysis

- Neutrino flux prediction shouldn't be tuned based on same neutrino data (e.g., MiniBooNE beam MC is based on external HARP measurement only).

- Precise background prediction is essential for precise cross section measurement (e.g., CC1π simultaneous measurement for CC1π background constraint in CCQE data sample).

- Experiments should provide reconstruction unbiased, efficiency corrected data, so that theorists can directly compare their models with experimental data (e.g., CCQE double differential cross section).

BooNE collaboration

University of Alabama
Bucknell University
University of Cincinnati
University of Colorado
Columbia University
Embry Riddle Aeronautical University
Fermi National Accelerator Laboratory
Indiana University
University of Florida

Los Alamos National Laboratory
Louisiana State University
Massachusetts Institute of Technology
University of Michigan
Princeton University
Saint Mary's University of Minnesota
Virginia Polytechnic Institute
Yale University

Grazie per la vostra attenzione!

Back up

MiniBooNE collaboration,
NIM.A599(2009)28

2. MiniBooNE detector

Timing cluster (subevent) distribution

Beam spill (1.6μs) is clearly evident.
Simple cut eliminate cosmic backgrounds

Beam and Cosmic BG

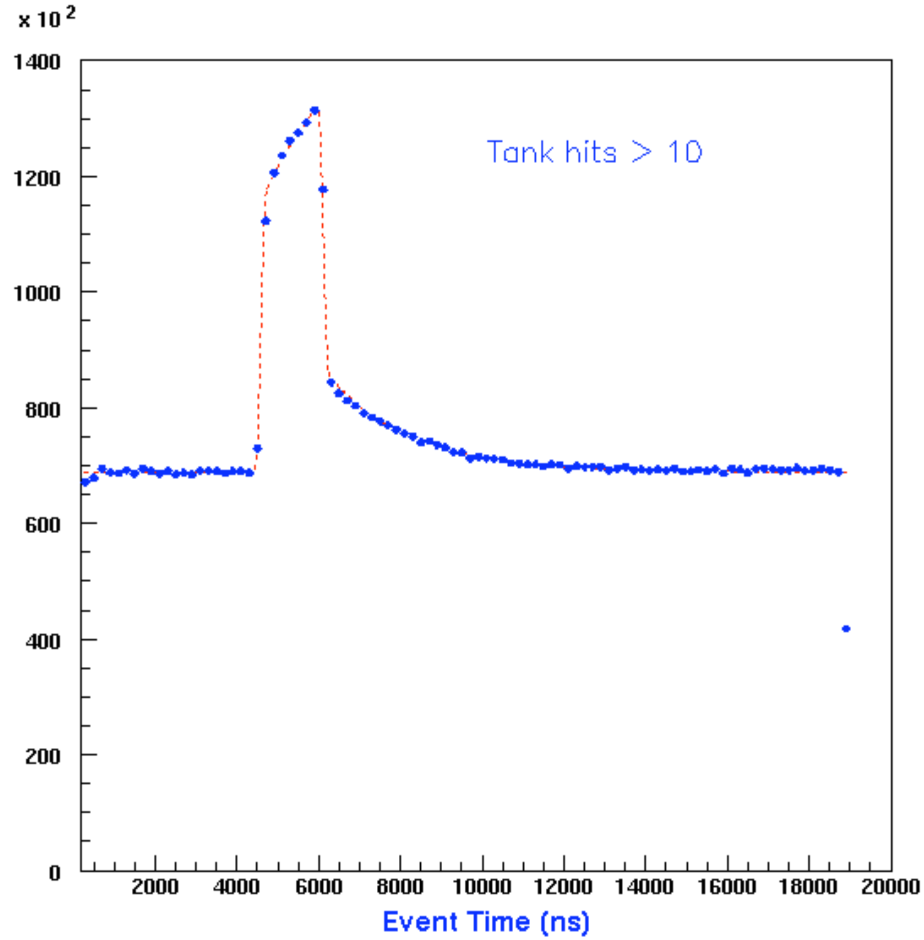

Neutrino candidate cuts

<6 veto PMT hits
Gets rid of cosmic muons

>200 tank PMT hits
Gets rid of muon-decay electrons

Only neutrino candidates are left!

MiniBooNE collaboration,
NIM.A599(2009)28

2. MiniBooNE detector

Timing cluster (subevent) distribution

Beam spill (1.6μs) is clearly evident.
Simple cut eliminate cosmic backgrounds

Neutrino candidate cuts

<6 veto PMT hits
Gets rid of cosmic muons

>200 tank PMT hits
Gets rid of muon-decay electrons

Only neutrino candidates are left!

Beam and Michels

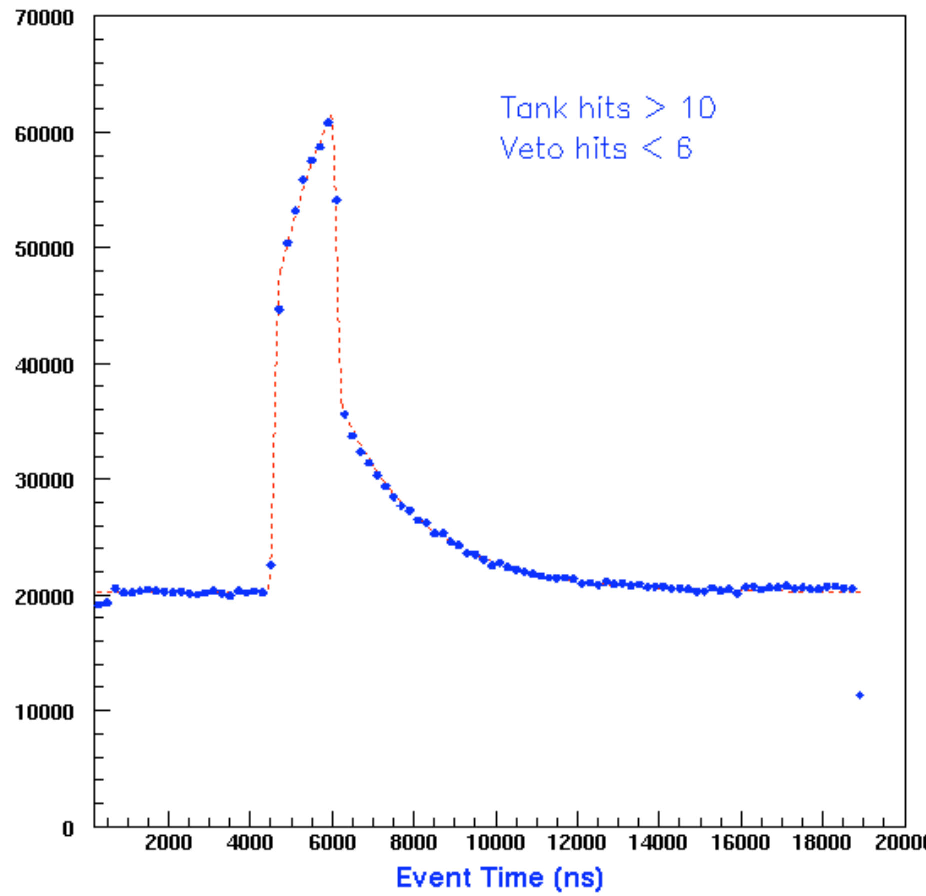

MiniBooNE collaboration,
NIM.A599(2009)28

2. MiniBooNE detector

Timing cluster (subevent) distribution

Beam spill (1.6μs) is clearly evident.
Simple cut eliminate cosmic backgrounds

Neutrino candidate cuts

<6 veto PMT hits
Gets rid of cosmic muons

>200 tank PMT hits
Gets rid of muon-decay electrons

Only neutrino candidates are left!

Beam Only

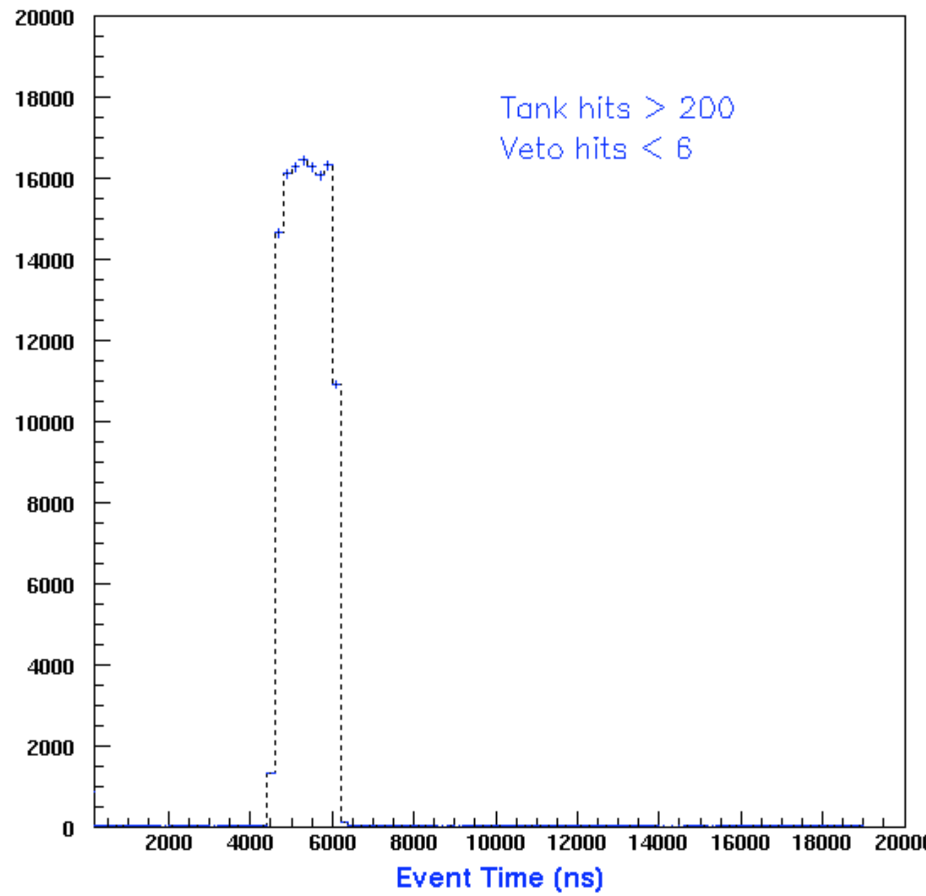

2. Energy scale of MiniBooNE

Mis-calibration of the detector can mimic large M_A value. Roughly, 2% of energy shift correspond to 0.1GeV change of M_A.

M_A-κ fit for 2% muon energy shifted data

To bring M_A=1.0GeV, 7% energy shift is required, but this is highly disfavored from the data.

Question is what is the possible maximum mis-calibration? (without using muon tracker data)

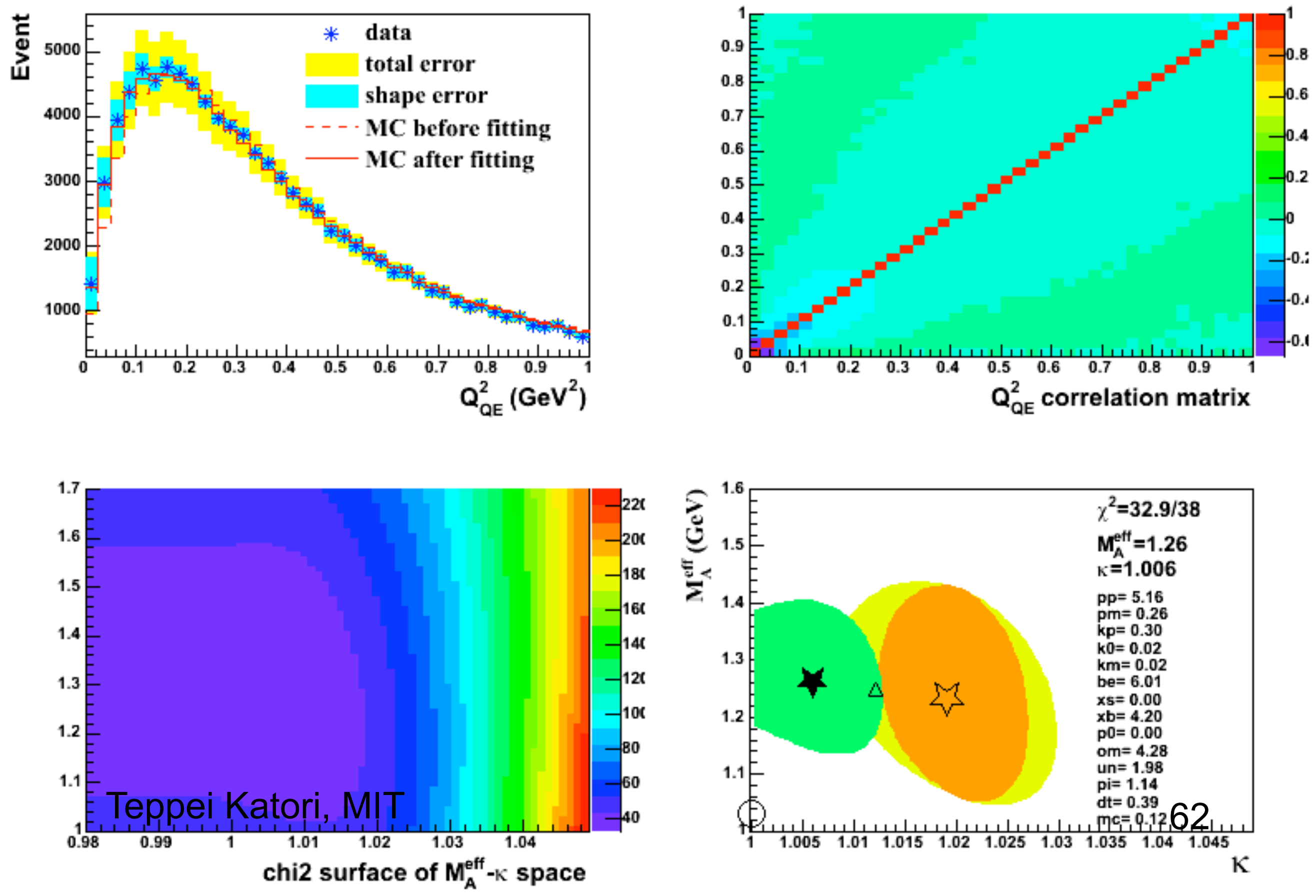

2. Energy scale of MiniBooNE

Range is the independent measure of muon energy. So range-T_μ difference for data and MC can be used to measure the possible mis-calibration.

This variable agrees in all energy regions within 2%.

Range - T_μ X 0.5+100 for (300-400MeV)

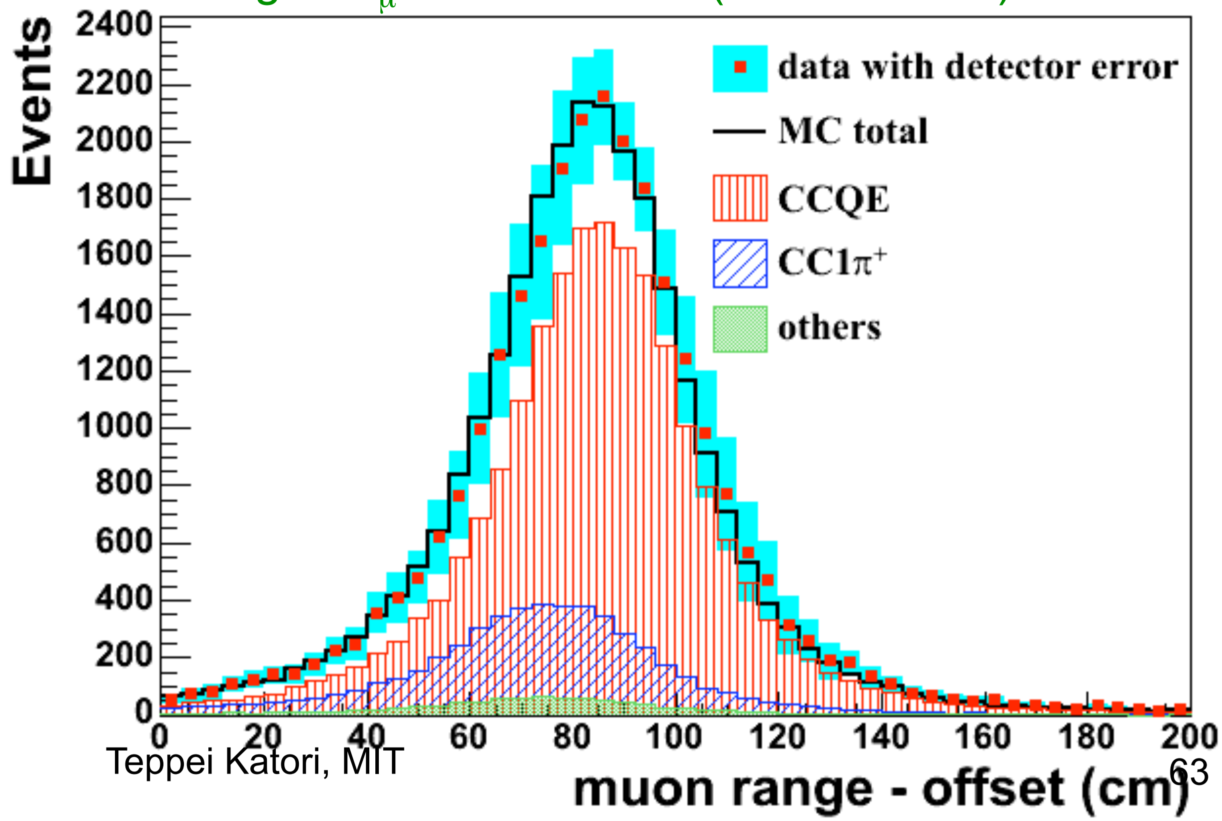

3. CC1π background constraint

This data driven MC tuning is based on 2 assumptions.

2. Pion absorption

The background subtraction is based on the assumption that our pion absorption model in the MC is right. To study this, we change the amount of pion absorption by a single number. Since pion absorption is the function of pion momentum, this is justified if pion momentum has week correlation with muon kinematics in CCπ event.

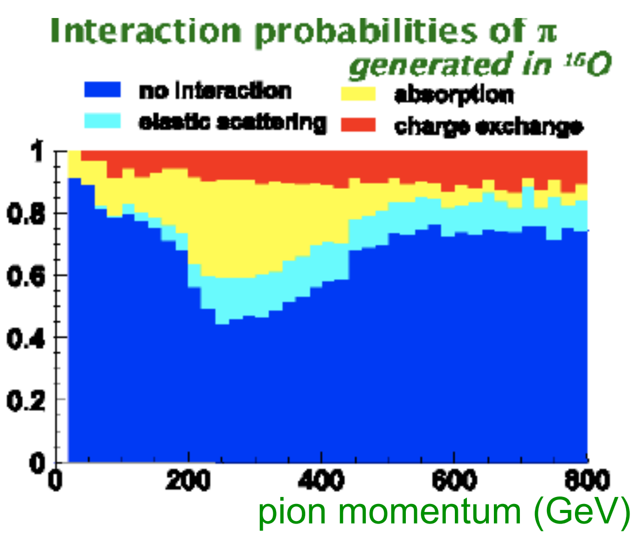

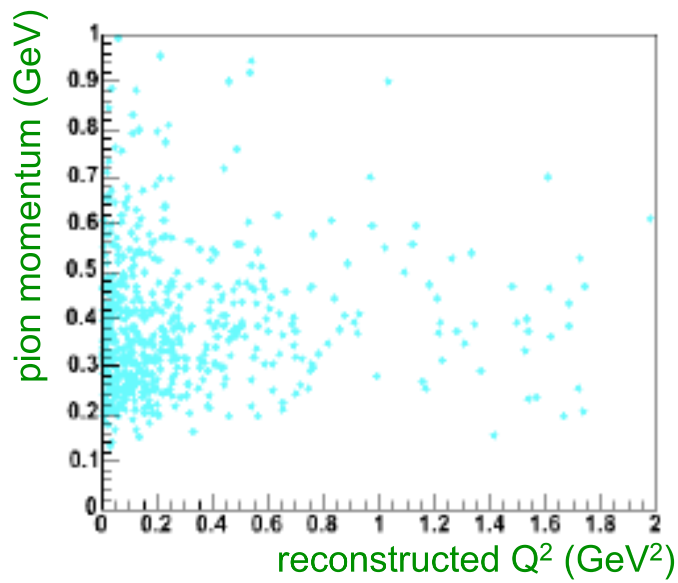

3. CC1π background constraint

This data driven MC tuning is based on 2 assumptions.

2. Pion absorption

The background subtraction is based on the assumption that our pion absorption model in the MC is right. To study this, we change the fraction of pion absorption.

Pion absorption is increased 0%, 15%, and 30%, meantime coherent fraction is decreased 0%, 50%, and 100%.

Any new xs models can provide good fit in 3 subevent sample in Q^2.

data-MC Q^2 ratio in 3 subevent

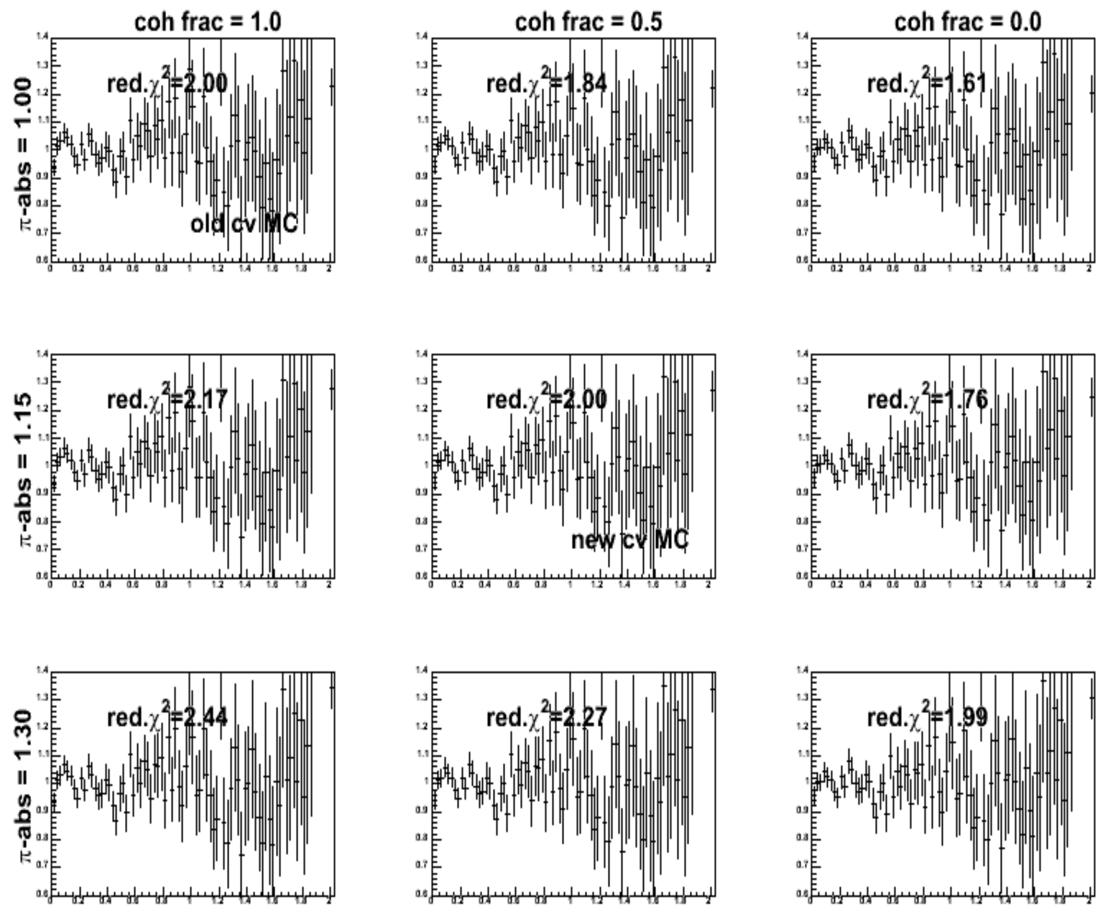

3. CC1π background constraint

This data driven MC tuning is based on 2 assumptions.

2. Pion absorption

However, we can differentiate xs models in T_μ-$\cos\theta_\mu$ plane.15% increase of piabs and 0% of coherent fraction gives the best fit.

We chose 15% for piabs, and 50% for cohfrac as new cv MC which will be used to estimate background from all kinematic distribution. This changes are well within our error (pion absorption 25%, charge exchange 30%). The rest of models go to make a new error matrix.

data-MC T_μ-$\cos\theta_\mu$ ratio in 3 subevent

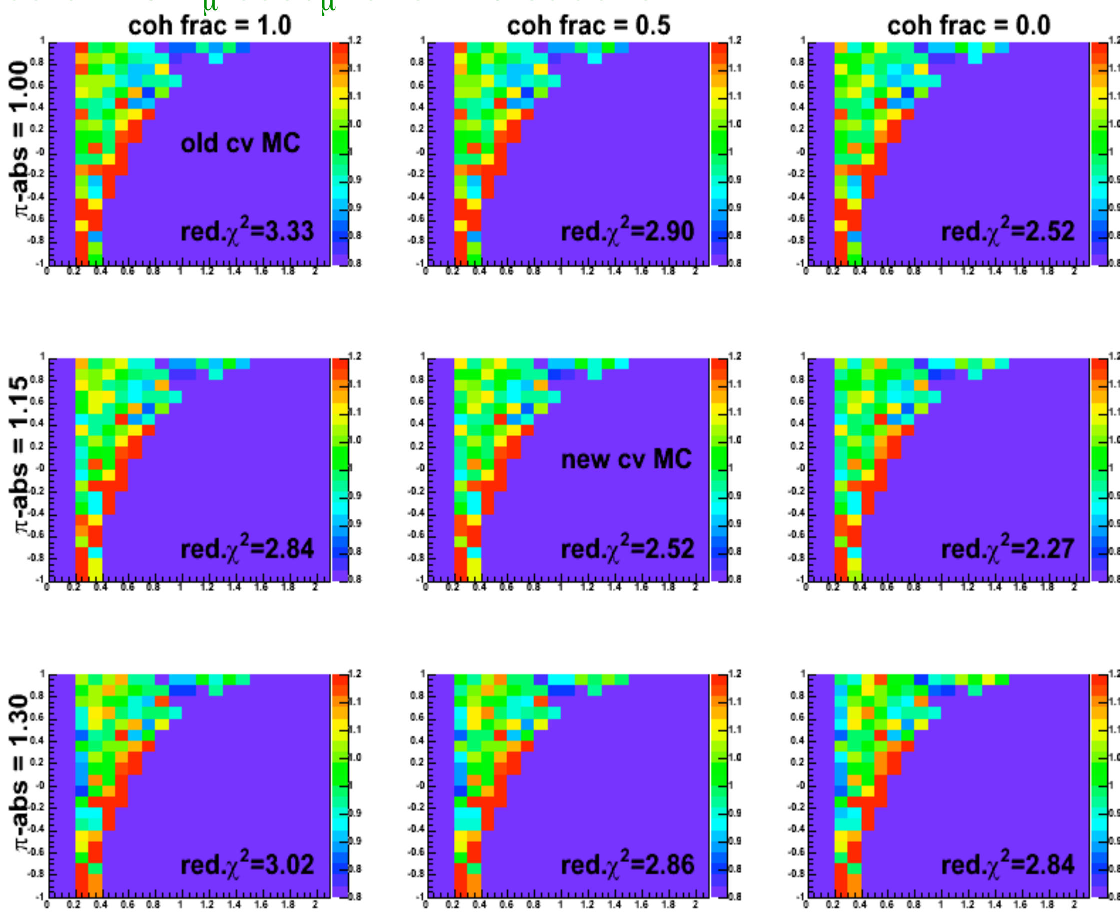

4. CC1π background constraint

This data driven MC tuning is based on 2 assumptions.

1. Kinematics measurement consistency between 2 and 3 subevent sample

Since 3 subevent has an additional particle (=pion), light profile is different. ~9% of events are misreconstructed to high Q^2 in 3 subevent, but majority of them are Q^2>0.5GeV^2, so they don't join the background subtraction.

2. Pion absorption

The background subtraction is based on the assumption that our pion absorption model in the MC is right. We assume 25% error for nuclear pion absorption, 30% for nuclear pion charge exchange, 35% for detector pion absorption, and 50% for detector pion charge exchange.
On top of that, we also include the shape error of pion absorption by change the fraction of resonance and coherent component.

MiniBooNE collaboration,
PRL100(2008)032301

5. Pauli blocking parameter "kappa", κ

We performed shape-only fit for Q^2 distribution to fix CCQE shape within RFG model, by tuning M_A^{eff} (effective axial mass) and κ

Pauli blocking parameter "kappa", κ

To enhance the Pauli blocking at low Q^2, we introduced a new parameter κ, which is the energy scale factor of lower bound of nucleon sea in RFG model in Smith-Moniz formalism, and controls the size of nucleon phase space

$$\mathrm{Elo} = \boxed{\kappa}\left(\sqrt{(p_F^2 + M^2)} - w + E_B\right)$$

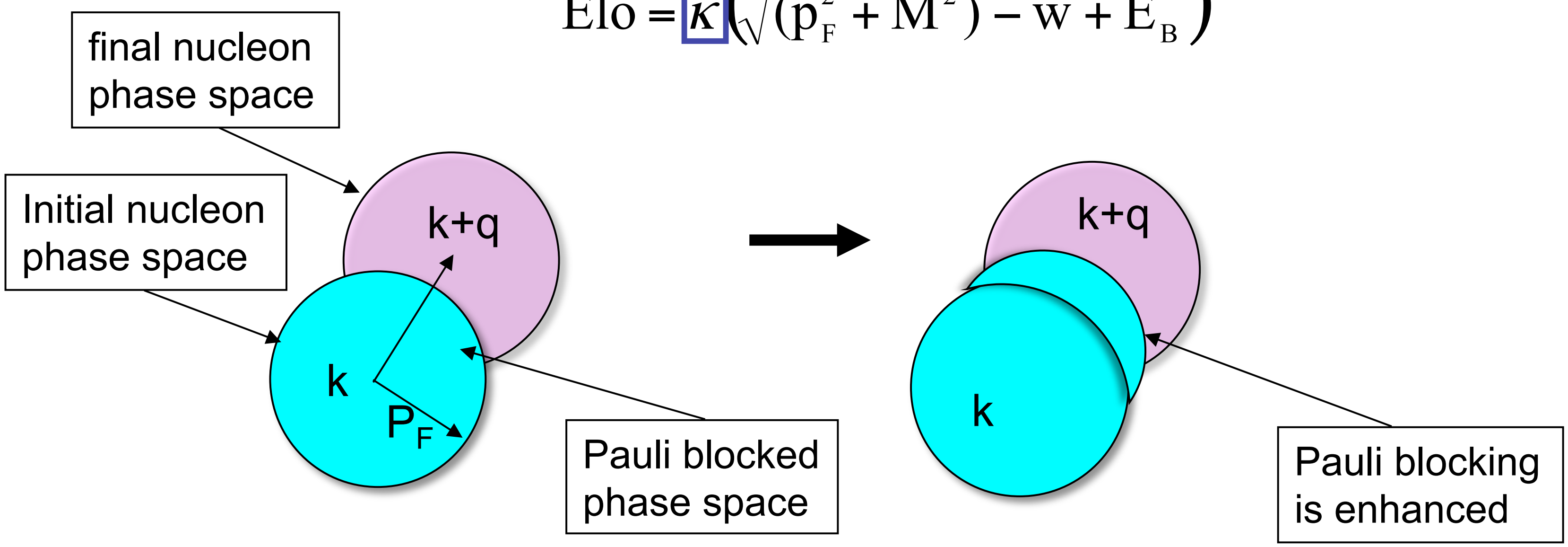

5. M_A^{eff}-κ shape-only fit

M_A^{eff} - κ shape-only fit result

M_A^{eff} = 1.35 ± 0.17 GeV (stat+sys)
κ = 1.007 $^{+0.007}_{-\infty}$ (stat+sys)
χ^2/ndf = 47.0/38

M_A^{eff} goes even up, this is related to our new background subtraction.

κ goes down due to the shape change of the background. Now κ is consistent with 1.
κ doesn't affects cross section below ~0.995.

Fit parameter space

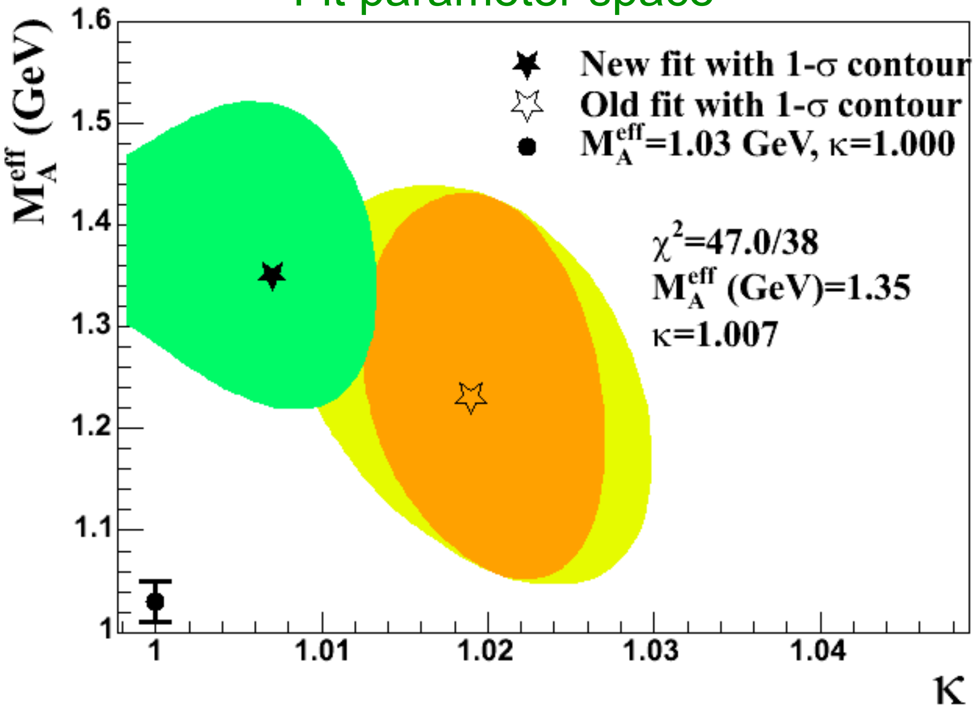

M_A^{eff} only fit M_A^{eff} = 1.37 ± 0.12 GeV χ^2/ndf = 48.6/39

Butkevich and Mikheyev,
Phys.Rev.C72:025501,2005

5. Kappa and (e,e') experiments

In low |q|, The RFG model systematically over predicts cross section for electron scattering experiments at low |q| (~low Q^2)

Data and predicted xs difference for ^{12}C

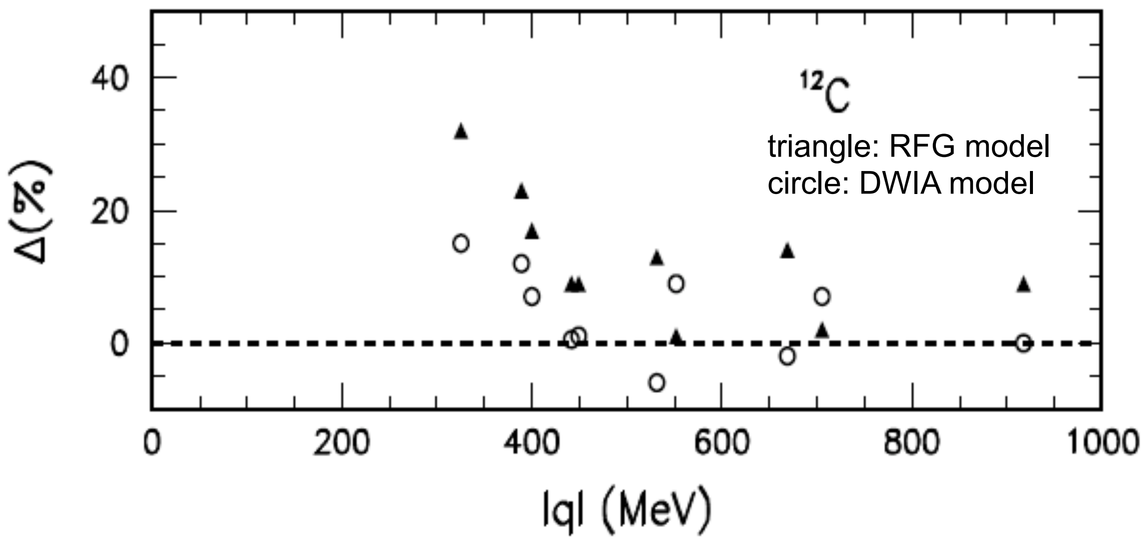

5. Kappa and (e,e') experiments

In low |q|, The RFG model systematically over predicts cross section for electron scattering experiments at low |q| (~low Q^2)

We had investigated the effect of Pauli blocking parameter "κ" in (e,e') data. κ cannot fix the shape mismatching of (e,e') data for each angle and energy, but it can fix integral of each cross section data, which is the observables for neutrino experiments. We conclude κ is consistent with (e,e') data.

black: (e,e') energy transfer data
red: RFG model with kappa (=1.019)
blue: RFG model without kappa

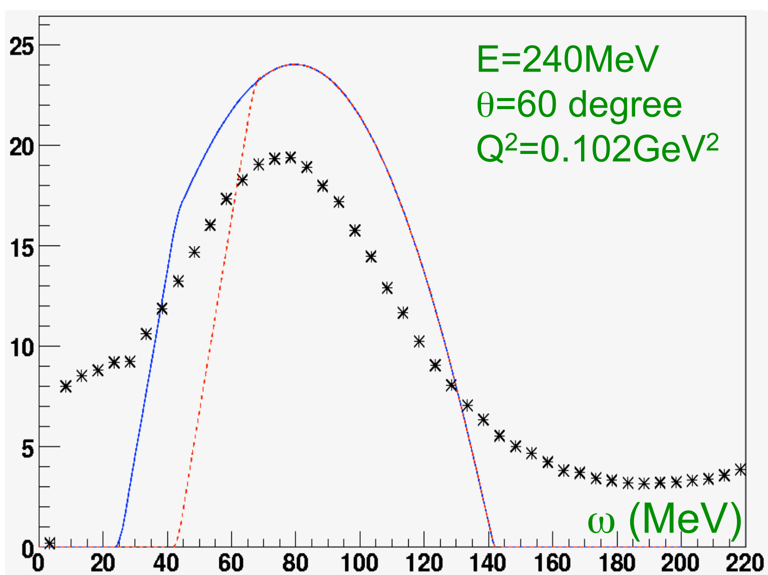

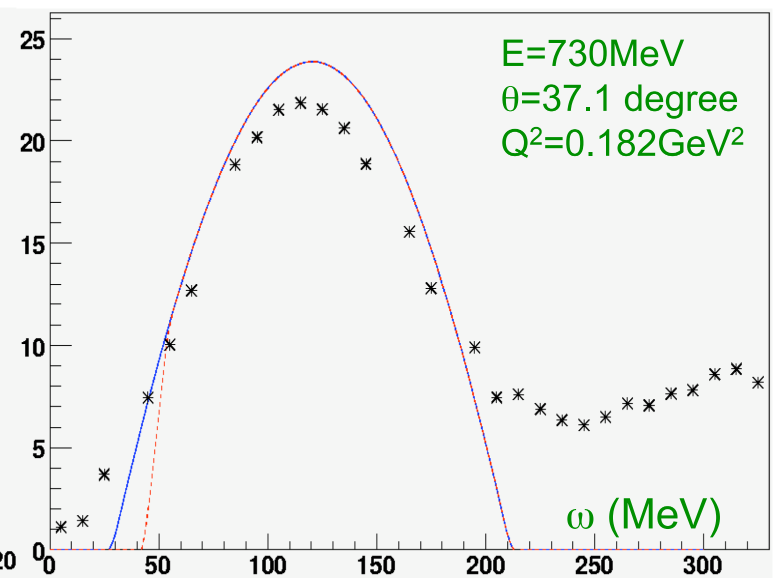

5. Kappa and (e,e') experiments

In low |q|, The RFG model systematically over predicts cross section for electron scattering experiments at low |q| (~low Q^2)

We had investigated the effect of Pauli blocking parameter "κ" in (e,e') data. κ cannot fix the shape mismatching of (e,e') data for each angle and energy, but it can fix integral of each cross section data, which is the observables for neutrino experiments. We conclude κ is consistent with (e,e') data.

RFG prediction-(e,e') data ratio in Q^2 (GeV^2)

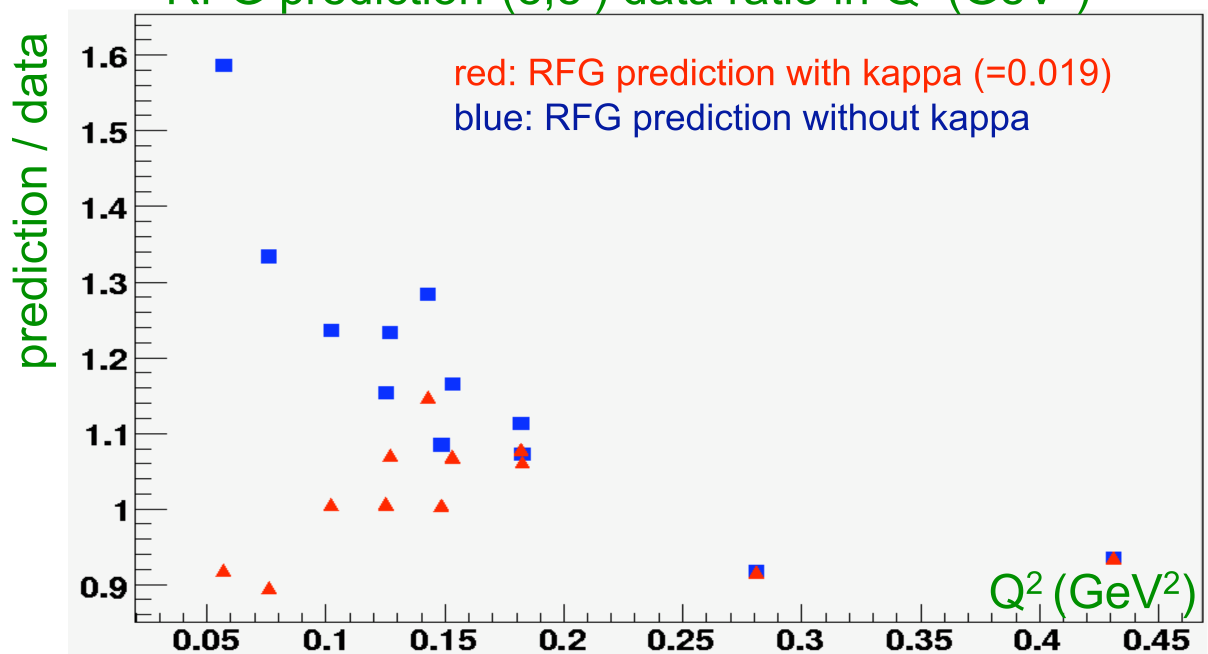

6. CCQE double differential cross section

Flux-integrated double differential cross section (T_μ-cosθ)

This is the most complete information about neutrino cross section based on muon kinematic measurement.

The error shown here is shape error, a total normalization error (δN_T=10.7%) is separated.

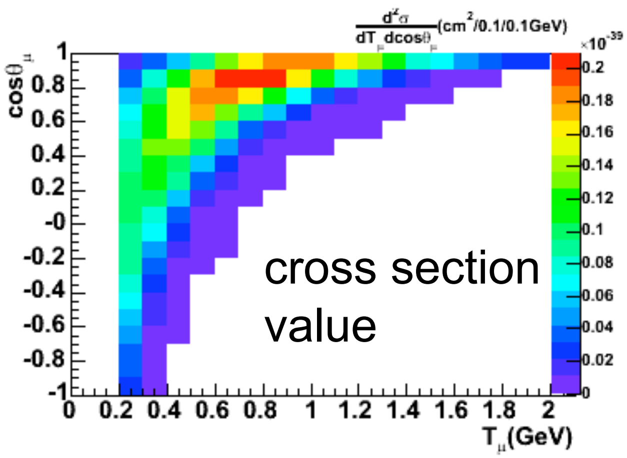

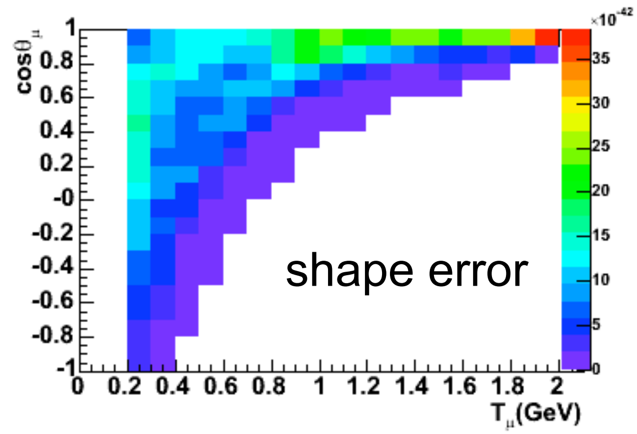

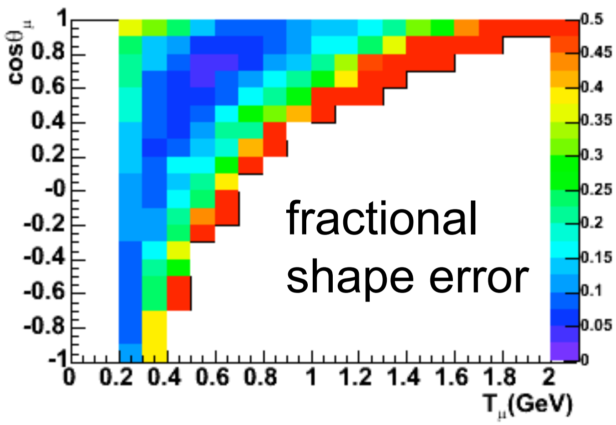

6. CCQE absolute cross section

Absolute flux-integrated differential cross section formula

i :true index
j : reconstructed index

The cross section is function of true value, for example, $d\sigma^2/T_\mu/\cos\theta_\mu$, $d\sigma/dQ^2_{QE}$, etc

Integrated flux is removed, so it is called flux-integrated cross section. If flux is corrected bin-by bin, it is called flux-unfolded cross section

$$\sigma_i = \frac{\sum_j U_{ij}\,(d_j - b_j)}{\varepsilon_i\,(\Phi T)}$$

U_{ij} :unsmearing matrix

d_j :data vector

b_j :predicted background

ε_i :efficiency

Φ :integrated ν-flux

T :integrated target number

6. CCQE absolute cross section

$$\sigma_i = \frac{\sum_j U_{ij} \boxed{(d_j - b_j)}}{\varepsilon_i \, (\Phi T)}$$

Absolute flux-integrated differential cross section formula

i :true index
j : reconstructed index

The predicted background (MC based on data driven tuning) is subtracted from data bin by bin (reconstructed bin)

MC also provide the distribution of irreducible background (have to be defined carefully).

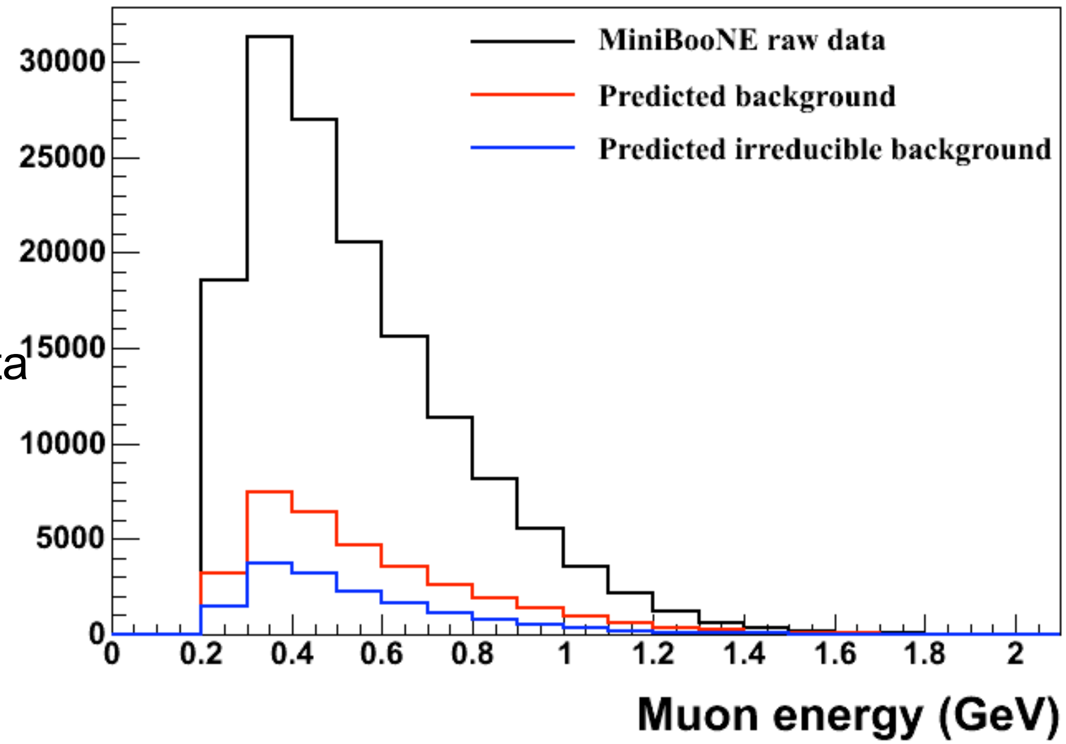

6. CCQE absolute cross section

D'Agostini, NIM.A362(1995)487

$$\sigma_i = \frac{\sum_j \boxed{U_{ij}} (d_j - b_j)}{\varepsilon_i (\Phi T)}$$

Absolute flux-integrated differential cross section formula

i :true index
j : reconstructed index

True distribution is obtained from unsmearing matrix made by MC. This technique is called “iterative Bayesian method” and known to be biased (discuss later).

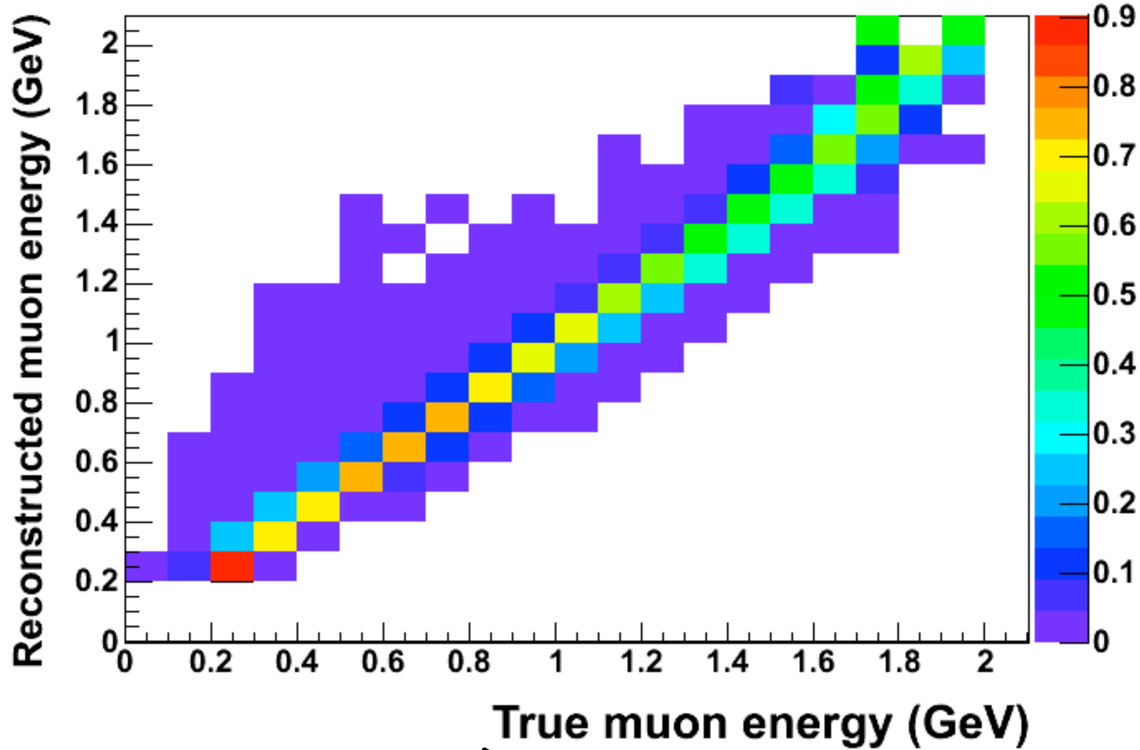

Notice, this unsmearing corrects detector effect of muon detection, and no nuclear model dependence.

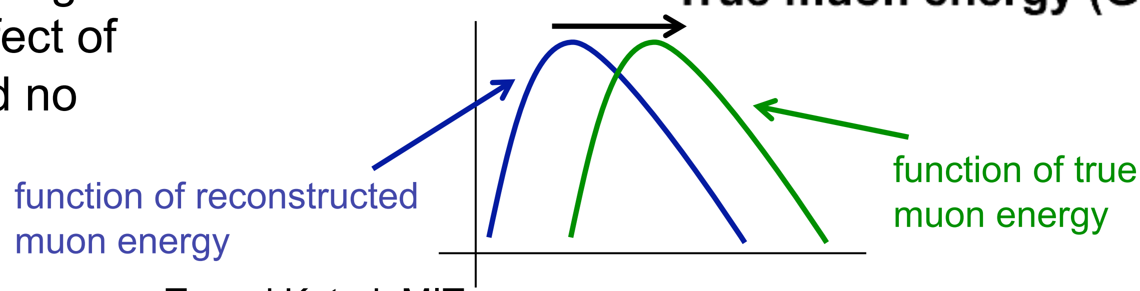

6. CCQE absolute cross section

D'Agostini, NIM.A362(1995)487

$$\sigma_i = \frac{\sum_j U_{ij}(d_j - b_j)}{\boxed{\varepsilon_i}(\Phi T)}$$

Absolute flux-integrated differential cross section formula

i :true index
j : reconstructed index

Then, efficiency is corrected bin by bin (true bin).

Again, efficiency correction correct detection efficiency of muon, and no nuclear model dependence.

Other word, if target distribution is reconstructed variable (Q^2, $E\nu$, etc), you have to be careful how these processes have been done.

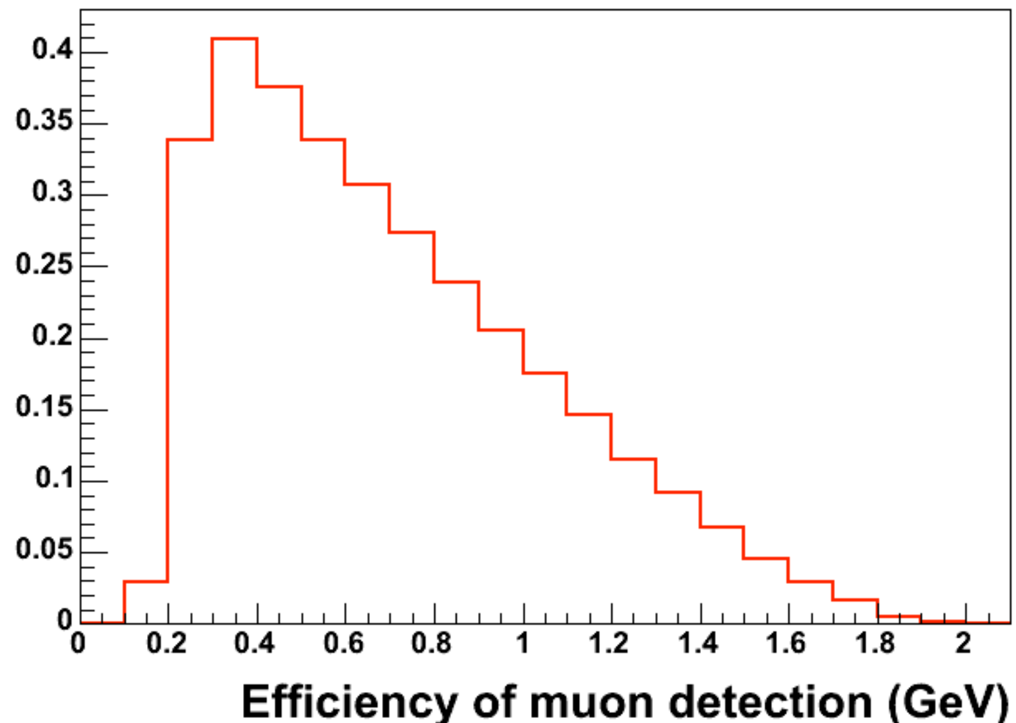

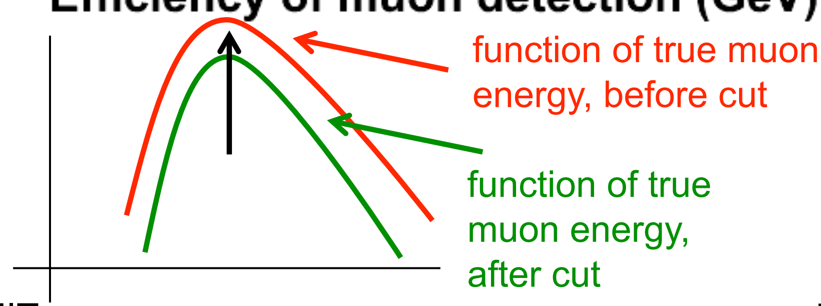

6. CCQE absolute cross section

D'Agostini, NIM.A362(1995)487

$$\sigma_i = \frac{\sum_j \boxed{U_{ij}} (d_j - b_j)}{\boxed{\varepsilon_i} (\Phi T)}$$

Absolute flux-integrated differential cross section formula

i :true index

j : reconstructed index

Then, efficiency corrected data is used to generate next unsmearing matrix (1st iteration). Any higher iteration gives ~same result.

Irreducible background is unfolded same way, by assuming efficiency is same.

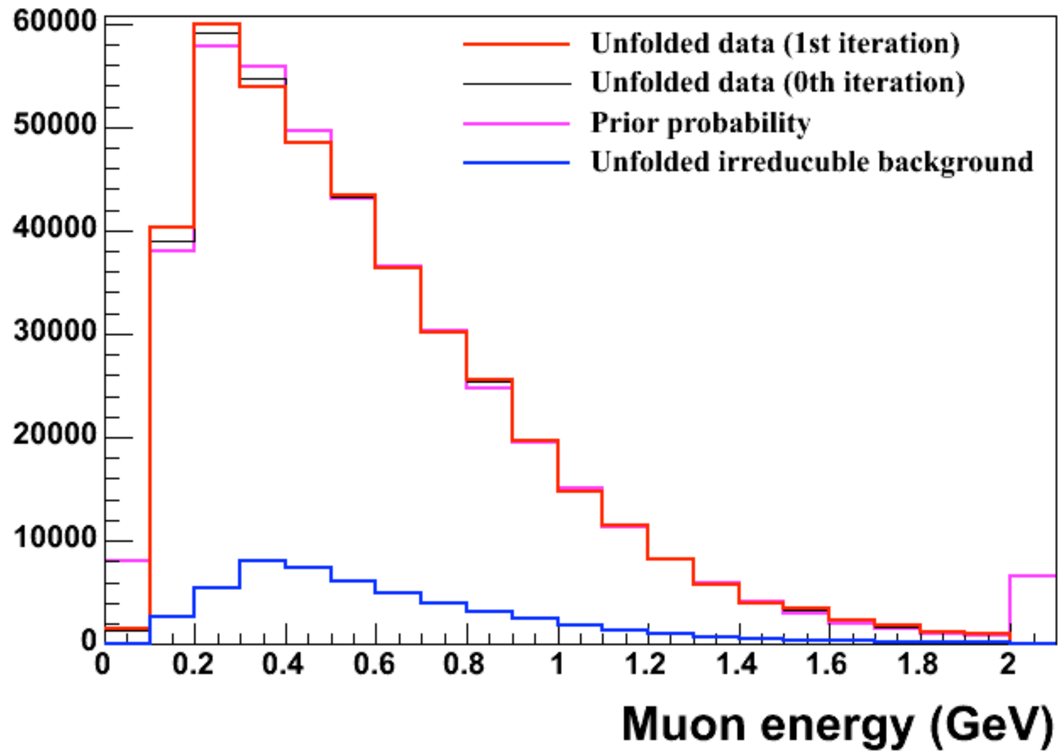

6. CCQE absolute cross section

$$\sigma_i = \frac{\sum_j U_{ij}(d_j - b_j)}{\varepsilon_i\,(\boxed{\Phi T})}$$

Absolute flux-integrated differential cross section formula

i :true index
j : reconstructed index

Finally, total flux and target number are corrected.

MiniBooNE flux prediction 100% rely on external beam measurement (HARP) and beamline simulation, and it doesn't depend on neutrino measurements by MiniBooNE.

Predicted ν_μ-flux in MiniBooNE

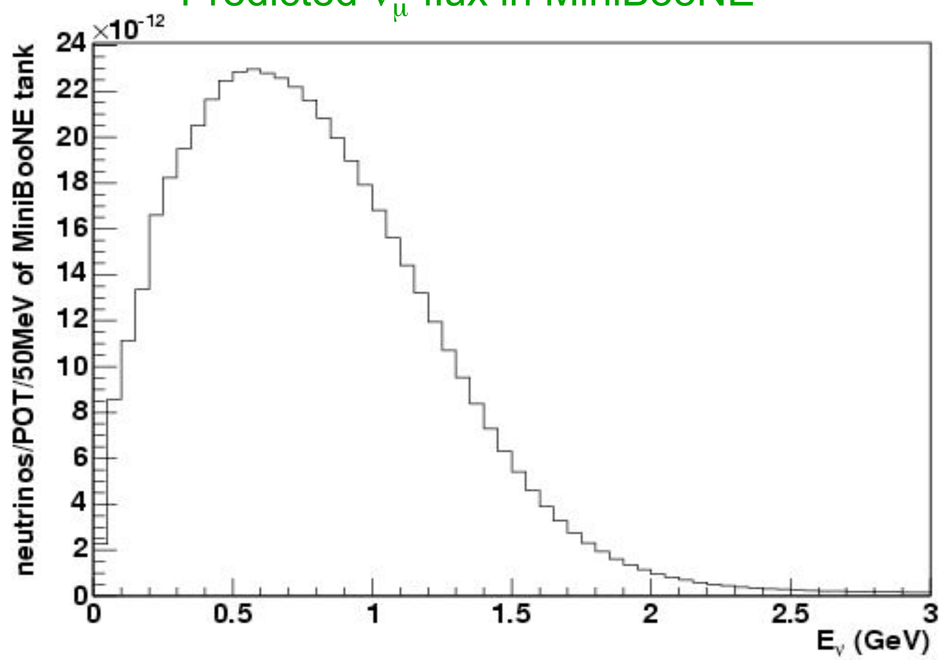

Flux Φ = integral of predicted ν_μ-flux
T = volume X oil density X neutron fraction

Jon Link, Nov. 18, 2005
Fermilab Wine & Cheese seminar

VOLUME 49, NUMBER 2 PHYSICAL REVIEW LETTERS 12 JULY 1982

Fermilab
15ft D_2 Bubble Chamber

Neutrino Flux and Total Charged-Current Cross Sections in High-Energy Neutrino-Deuterium Interactions

T. Kitagaki, S. Tanaka, H. Yuta, K. Abe, K. Hasegawa, A. Yamaguchi, K. Tamai, T. Hayashino, Y. Ohtani, and H. Hayano
Tohoku University, Sendai 980, Japan

To obtain the total cross section from the number of events, the neutrino flux has to be measured on an absolute scale. In this analysis, we determine the neutrino flux using 362 quasielastic events identified in our data[10] and the cross section for reaction (2) derived from the $V-A$ theory.

Again, they use QE events and theoretical cross section to calculate the ν.

When they try to get the flux from meson (π and K) production and decay kinematics they fail miserably for E_ν<30 GeV.

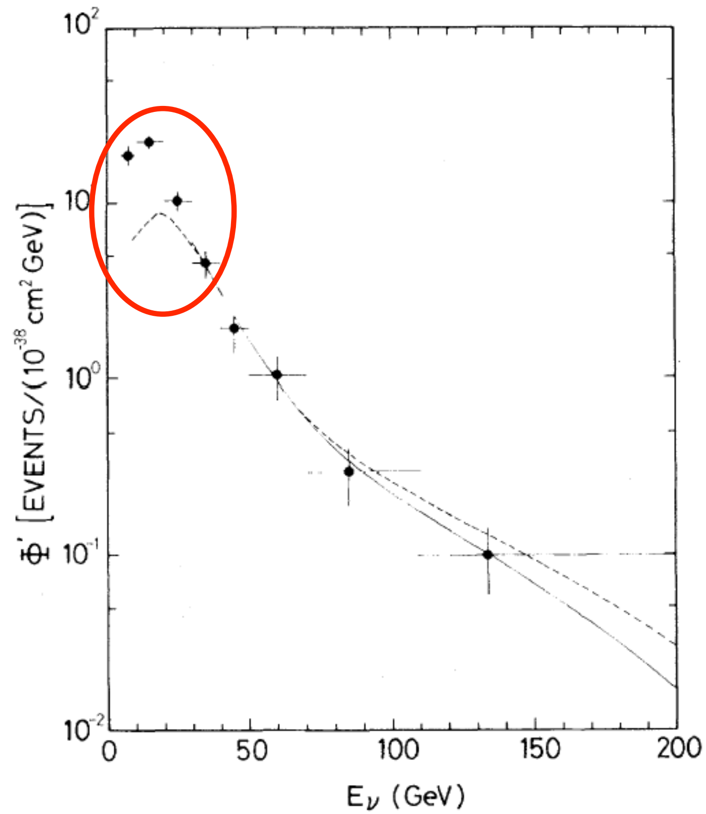

FIG. 2. Neutrino flux distribution obtained from the quasielastic events and the predicted cross section with M_A = 1.05 GeV. The solid curve is obtained from the best fit to the flux data for E_ν > 30 GeV. The dashed curve is taken from the Monte Carlo simulation of the flux.

Jon Link, Nov. 18, 2005
Fermilab Wine & Cheese seminar

PHYSICAL REVIEW D VOLUME 23, NUMBER 11 1 JUNE 1981

Quasielastic neutrino scattering: A measurement of the weak nucleon axial-vector form factor

N. J. Baker, A. M. Cnops,* P. L. Connolly, S. A. Kahn, H. G. Kirk, M. J. Murtagh, R. B. Palmer, N. P. Samios, and M. Tanaka

Brookhaven National Laboratory, Upton, New York 11973

(Received 12 February 1981)

Brookhaven AGS

7ft D_2 Bubble Chamber

The quasielastic reaction $\nu_\mu n \to \mu^- p$ was studied in an experiment using the BNL 7-foot deuterium bubble chamber exposed to the wide-band neutrino beam with an average energy of 1.6 GeV. A total of 1138 quasielastic events in the momentum-transfer range $Q^2 = 0.06-3.00$ $(\mathrm{GeV}/c)^2$ were selected by kinematic fitting and particle identification and were used to extract the axial-vector form factor $F_A(Q^2)$ from the Q^2 distribution. In the framework of the conventional $V-A$ theory, we find that the dipole parametrization is favored over the monopole. The value of the axial-vector mass M_A in the dipole parametrization is 1.07 ± 0.06 GeV, which is in good agreement with both recent neutrino and electroproduction experiments. In addition, the standard assumptions of conserved vector current and no second-class currents are checked.

We have used a maximum likelihood method to extract M_A from the shape of the Q^2 distribution for each observed neutrino energy. This likelihood function $\mathcal{L}^I$ is independent of the shape of the neutrino spectrum ...

They didn't even try to determine their ν flux from pion production and beam dynamics.

Phys. Rev. D **25**, 617 (1982)

The distribution of events in neutrino energy for the 3C $\nu d \to \mu^- p p_s$ events is shown in Fig. 4 together with the quasielastic cross section $\sigma(\nu n \to \mu^- p)$ calculated using the standard $V-A$ theory with $M_A = 1.05 \pm 0.05$ GeV and $M_V = 0.84$ GeV. The absolute cross sections for the CC interactions have been measured using the quasielastic events and its known cross section.[4]

In subsequent cross section analyses the theoretical ("known") quas-ielastic cross section and observed quasi-elastic events were used to determine the flux.

Jon Link, Nov. 18, 2005
Fermilab Wine & Cheese seminar

PHYSICAL REVIEW D VOLUME 34, NUMBER 1 1 JULY 1986

Determination of the neutrino fluxes in the Brookhaven wide-band beams

L. A. Ahrens, S. H. Aronson, P. L. Connolly,* B. G. Gibbard, M. J. Murtagh, S. J. Murtagh,†
S. Terada, and D. H. White
Physics Department, Brookhaven National Laboratory, Upton, New York 11973

Brookhaven AGS

Liquid Scintillator

The beam calculations described here were based on the Grote, Hagedorn, and Ranft (GHR) (Ref. 11) parametrization; that of Sanford and Wang was used for comparison. An estimate was made of pion production by reinteracting protons guided by the shape of the observed ν_μ spectrum and the observed angular distribution of muons from quasielastic events. The procedure is described[12] in the Appendix.

The Procedure

- Pion production cross sections in some low momentum bins are scaled up by 18 to 79%.
- The K^+ to π^+ ratio is increased by 25%.
- Overall neutrino (anti-neutrino) flux is increased by 10% (30%).

All driven by the neutrino events observed in the detector!

Jon Link, Nov. 18, 2005
Fermilab Wine & Cheese seminar

PHYSICAL REVIEW D VOLUME 16, NUMBER 11 1 DECEMBER 1977

Argonne ZGS

12ft D_2 Bubble Chamber

Study of neutrino interactions in hydrogen and deuterium: Description of the experiment and study of the reaction $\nu + d \rightarrow \mu^- + p + p_s$†

S. J. Barish,* J. Campbell,‡ G. Charlton,§ Y. Cho, M. Derrick, R. Engelmann,‖ L. G. Hyman, D. Jankowski, A. Mann,¶ B. Musgrave, P. Schreiner, P. F. Schultz, R. Singer, M. Szczekowski,** T. Wangler, and H. Yuta††
Argonne National Laboratory, Argonne, Illinois 60439

Flux derived from pion production data. Were able to test assumptions about the form of the cross section using absolute rate and shape information.

TABLE IV. Results of axial-form-factor fits.

Likelihood function	M_A^{Dipole} (GeV)	M_A^{Monopole} (GeV)	M_A^{Tripole} (GeV)
Rate	$0.75^{+0.13}_{-0.11}$	$0.45^{+0.11}_{-0.07}$	$0.96^{+0.17}_{-0.14}$
Shape	1.010 ± 0.09	0.56 ± 0.08	1.32 ± 0.11
Rate and shape	0.95 ± 0.09	0.52 ± 0.08	1.25 ± 0.11
Flux independent	0.95 ± 0.09	0.53 ± 0.08	1.25 ± 0.11

- Pion production measured in ZGS beams were used in this analysis
- A very careful job was done to normalize the beam.
- Yet they have a 25% inconsistency between the axial mass they measure considering only rate information verses considering only spectral information.

Interpretation: Their normalization is wrong.